Working Area Data Assimilation

Progress Report

Prepared by:	Area Leader Antonín Bučánek
Period:	Q1,Q2 2026
Date:	11/09/2026

Progress summary

The report summarizes the RC LACE DA activities in Q1–Q2 2026. It focuses on the use of observational data—particularly all-sky and clear sky satellite assimilation, radar, Mode-S, and GNSS ZTD—as well as on the implementation and refinement of hourly assimilation systems designed to support NWP-based nowcasting and surface data assimilation.

The research and development on radar data assimilation has a goal to enhance the realism of modeled precipitation patterns in the initial hours of the NWP forecast. Two scientific stays on radar data assimilation were executed. One stay was focusing on tuning of direct assimilation in 3DEnvar method. The second one was focusing on use of radar Doppler winds.

Work on the assimilation of satellite observations continued, with the main focus on integrating the all-sky approach into a unified framework. The all-sky assimilation of MTG FCI infrared radiances was successfully implemented and tested. Parallel work focused on advancing all-sky IASI assimilation in the C-LAEF 1k system using the Okamoto method, as preparatory work for the future MTG IRS sounder.

A bugfix in the pre-thinning of Mode-S EHS data allowed the correct reading of all available observations from BUFR files before the pre-thinning step. Additionally, a new whitelist was created for EMADDC EHS data. Currently, the assimilation of EHS and MRAR data using the adaptive weighting method is being evaluated in AROME/HU.

Research and development on ensemble variational (EnVar) assimilation continued. The 3DEnVar system was evaluated using sub-ensembles and variance scaling switches in CY48t3bf3, revealing that horizontal localization length impacts spread more significantly than variance scaling. Additionally, verification from summer 2026 demonstrated that 3DEnVar consistently improves surface variables up to 60 hours and precipitation up to 12 hours compared to the 3D-Var control, despite a shared overestimation of heavy rainfall (see section DA6).

Work on surface data assimilation progressed in several areas. A snow analysis was operationally implemented at CHMI in May 2026 with retuned snow fractions to mitigate surface cooling. New national Swiss snow data were added to AROME-RUC/AT. First test of 2DEnVar for screen-level data in the Claef Alpe-Adria successfully produced terrain-dependent increments, though they are currently overly localized around observation sites. For the ALARO+SURFEX OI setup, technical bugs were resolved to enable stable execution of the CANARI scheme with SURFEX, allowing high-resolution validation experiments to get underway.

Last but not least, the first steps were taken to familiarize with the new C++ layer of the ACCORD/ALADIN code, which was earlier successfully ported and used to reproduce the current 3D-Var assimilation.

Actions/Subjects/Deliverables

Subject: *Operational implementation of DA systems [COM3]*

Description and deliverables:

An overview of the current operational DA systems in RC LACE countries are presented in the following two tables (yellow colors indicate the system upgrades and additions made):

Table E1: Operational DA for NWP systems run by RC LACE countries.

DA	AUSTRIA AROME	CROATIA ALARO	CZECH REP. ALARO	HUNGARY ALARO	HUNGARY AROME	SLOVAKIA ALARO	SLOVENIA ALARO
Resol	2.5L90, 600 x 432	4.0L73 480 x 432	2.3L87-NH 1069 x 853	8L49 349x309	2.5L60 490x310	4.5L87 625x576	4.4L87 432 x 432
Cycle	43t2bf11+loc.	43t2bf10	46t3mas_op1.09	cy40t1	cy46t1bf07	cy46t1bf07	43t2bf10
LBC	IFS 1h (lagged)	IFS 1h (lagged)	ARP 3h	IFS 3h (lagged)	IFS 1h (lagged)	ARP 3h	IFS 1h/3h (lagged)
Method	OI_main MESCAN + 3d-Var	OI + 3D-Var + Jk	OI + BlendVar	OI + 3D-Var	SEKF + 3D-Var	BlendVar + OI	OI + 3D-Var
Cycling	3h	3h	3h	6h	3h	6h	3h
B matrix	EDA on C-LAEF	EDA	EDA	EDA	EDA	Downscaled AEARP	Downscaled ECMWF ENS
Initiali-zation	No (SCC)	No (SCC)	IDFI in pro-duction, SCC	DFI	No	No	No (SCC)
Obs.	Synop + AS, Amdar/MRAR /EHS-EU, AMV, Temp, ASCAT, Snow-grid/MODIS, snowmask, Ceilometer	Synop, Amdar/MRAR, AMV, Temp, Seviri, Radar RH (OPERA),	Synop + AS, Amdar/MRAR /EHS-EU, HRW, Profiler, Temp, ASCAT, Seviri, Radar Refl. (OPERA), Snow analysis	Synop + AS, Amdar, AMV, Temp, Seviri, AMSUA/MHS,	Synop + AS, GNSS ZTD, Amdar/MRAR, Temp, AMV+HRW,	Synop + AS TEMP HRW AMDAR + Mode-S ZTD	Synop + AS Amdar/MRAR/ EHS, AMV, Temp Seviri, AMSUA/MHS/ IASI, ASCAT/OSCAT, E-GVAP ZTD (passive)
Cut-off (prod / assim)	1:45h			3h	1:30h	2:35 / 7:45h	2:15 / 4:00h

Table E2: Operational DA for NWP-based nowcasting systems at hourly scale run by the RC LACE countries.

DA	AUSTRIA AROME RUC	CZECH REP. VarCanPack	SLOVENIA ALARO-RUC
Resol	1.2L90 900 x 576	2.3L87-NH 1069 x 853	1.3L87 589x589
Cycle	43t2bf11	46t3mas_op1.09	cy43t2bf10
LBC	AROME-Aut 2.5km 1h	-	ECMWF 1h
Method	OI_main MESCAN + 3d-Var + LHN + FDDA +IAU	3DVAR + OI	3D-Var + OI
Cycling	1h	-	1h
B matrix	Static EDA + differences of the day	EDA	static DSC ENS
Initialization	IAU		No (SCC)
Obs	Synop + AS, Amdar (q)/MRAR/EHS national, EHS-EU, AMV/HRW, bufrTemp, Seviri, AMSUA/MHS/HIRS/ATMS/IASI (+ Metop-C), ASCAT, GNSS ZTD (Austria + EGVAP 1h VarBC), GPSRO (ROMSAF/OPLACE), Radar RH/Dow, INCA + AS at hig.freq., MODIS snowmask, windfarms, celiome-ters, Profiler, towers, NOAA20 JPSS ATMS, NOAA21 ATMS, More snow from Swiss	Synop + AS, Amdar/MRAR/EHS-EU, HRW, Profiler, ASCAT, Seviri	SYNOP + AWS, AMDAR/ MRAR/ EHS, AMV, TEMP, SEVIRI, AMSU-A/MHS/IASI, ASCAT/OSCAT, radar reflectivity

Cutoff	0:27		0:35/1:10

Table E3: Operational ensemble systems in RC LACE countries that include the DA component.

DA	C-LAEF_AlpeAdria (AT, HR, SI)	HUNGARY AROME-EPS	LACE A-LAEF
Resol.	1.0L90, 1500x1350	2.5L60, 490 x 310	4.8L60, 1250 x 750
Cycle	46t1 export +local changes and LACE RADAR modset (cy48t3bf3+ OOPS for EnVar part only)	cy46t1bf07	40t1 + loc.changes
members	15+1+1EnVar	10+1	16+1
LBC	IFS-1h (Backup Arpège)	IFS ENS 1h (lagged)	IFS 6h (lagged)
Method	3D-Var+ensemble Jk+OI perturbed obs (1 member 3D-EnVar)	3D-Var + SEKF	DF blending + ESDA
Cycling	3h; long forecast only from a few member every 3h	3h	12h
B matrix	static full C-LAEF_AA EDA	Static EDA	-
Additional Initialization	No	No	No
Obs.	SYNOP, AMDAR/MODE-S(KNMI-EU OPLACE)/MRAR-OPLACE, AMV, TEMP, ASCAT25km, ceilometers, GNSS-ZTD, RADAR reflectivities	SYNOP + AWS, GNSS ZTD, AMDAR/MRAR, TEMP, AMV+HRW	Synop + AS
Obs. cutoff	1:45	1:30	1:00

In **Austria**, a 1 km version of C-LAEF_AA (CLAEF Alpe Adria) is made operational. The system consists from 15 EDA members, 1 control member +1 EnVar member. C-LAEF_AA is completely based on cy46t1 while the EnVar member is on cy48t3. Observations and other settings are mostly as in C-LAEF, GNSS-ZTDs data with revised whitelist and RADAR reflectivity data with Slovenian setting are used. Main focus of works is tuning the EnVar member and AllSky assimilation.

In the **Czech Republic**, OPERA radar reflectivity assimilation was made operational in May 2025. A new cycle, cy48t3 with local modifications (cy48t3mas), became operational at the beginning of 2026. This was followed at the end of May 2026 by the implementation of snow analysis into the operational chain, which added national snow observations from AT, HU, and CH in addition to the standard GTS data. In September 2026, new national synoptic data from HR, SK, and SI, along with a revised blacklisting, was integrated into the operational system.

In **Croatia**, work is continuing on all-sky assimilation of IASI, and DHMZ has joined the CLAEF Alpe-Adria project. Additionally, preparatory work for a high-resolution configuration is currently ongoing.

In **Hungary**, OPLACE national synoptic observations were re-tuned, and a new whitelist for GNSS ZTD was created due to the availability of new GNSS observations. EMADDC MRAR/EHS data have been preprocessed and are now being validated for inclusion in the AROME and AROME RUC e-suite.

In **Slovakia**, two ALARO-1 configurations are pre-operational, both featuring a 1 km resolution and 87 vertical levels (L87) based on cycle cy46t1bf07. While both configurations utilize 3D-Var data assimilation, they differ in their setup: RUC1 runs hourly using lagged boundary conditions, whereas ALA1 runs on a 6-hour cycle and incorporates OPERA radar reflectivity data.

In **Slovenia**, HOOF preprocessing rewritten to C++ lead to significant speed improvement, the new C++ version runs 6-8 times faster. ARSO also part of the CLAEF Alpe-Adria project, focusing on tuning of Envar member.

In **Romania**, there are ongoing efforts to set up data assimilation cycling with CANARI with promising results.

In **Poland**, the activities towards the first assimilation suite are ongoing.

Contributors: All (approx. 1 PM per country, more in some institutes)

Subject: ***In-situ observations [DA1]***

Description and objectives:

Implementation of high-resolution ascent and decent radiosondes and wind profilers: optimize local pre-processing, extend observation operator, assess the quality and perform impact study. (DA1.1)

No work reported.

Surface observations (Ps, T2m, Hu2m, V10m): Perform impact assessment of high-quality and high-resolution SYNOP DA (DA1.2)

Testing additional SYNOP data in AROME/HU 3D-Var

From the surrounding countries, we currently use only those SYNOP observations in our AROME/HU operational system that are available through the GTS, and we would like to expand it with data from their national OBSOUL files. **Anikó Kardos-Várkonyi (HU)** carried out experiments at 2.5kmL60 and 1.3kmL90 resolutions with 3-hourly and 1-hourly assimilation cycles, respectively. The evaluation covered two periods: the entire month of April 2025 and the period from 22 October to 20 November 2025. The number of assimilated SYNOP data roughly doubled due to the extra input data (Figure 1). The OMG and OMA values showed a slight increase for all parameters.

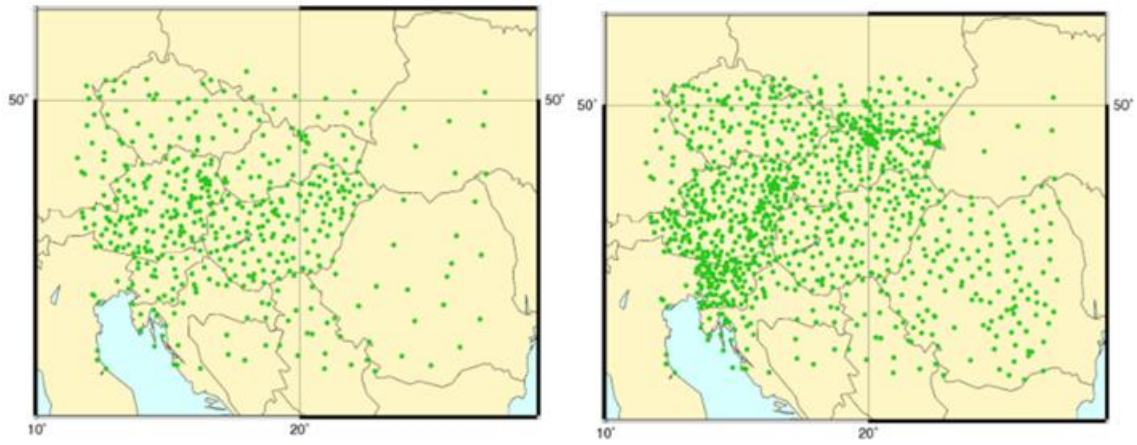


Figure 1: 2-metre temperature SYNOP data used in the assimilation system of the current operational AROME/HU (left) and in the experiments with additional SYNOP data (right).

Based on the verification, the results varied significantly by resolution and by time period. In the case of 2.5kmL60 with a 3-hourly assimilation cycle, a slight improvement can be observed for several parameters, although in many cases the results were neutral. The operational analysis and forecast for the first few hours were more accurate, while the experimental setting produced better results during the second half of the forecast range, especially in bias (Figure 2, left). Furthermore, in the case of 1.3kmL90, the assimilation of additional SYNOP data generally had a neutral or slightly

positive effect, but in some cases a degradation was also observed. For the 2-metre temperature, the improvements were less significant than in the 2.5kmL60 experiment (Figure 2). There were several instances in which differing precipitation fields or low-level cloud cover caused larger temperature differences. The current experiments were achieved with applying a dedicated blacklist for the additional data. We believe that more positive impact could be gained with its reconsideration, thus we are going to continue the tests in this direction. (1.75 PM)

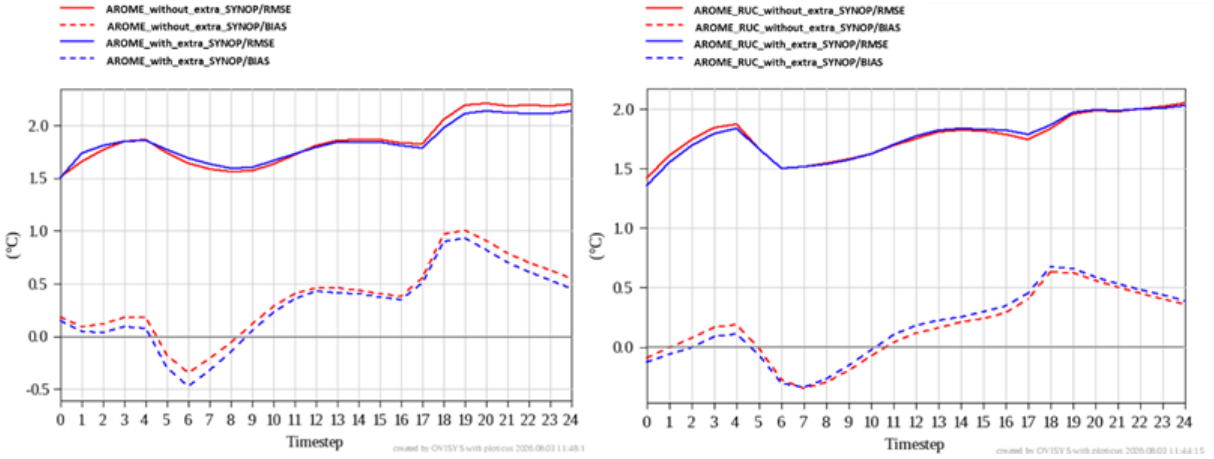


Figure 2: Bias (dashed) and RMSE (solid) of 2-metre temperature forecast in function of lead time [h] over the AROME/HU domain. Left: experiment at 2.5kmL60 with 3-hourly cycling assimilating additional SYNOP data (blue) and the corresponding reference run (red). Right: experiment at 1.3kmL90 with hourly cycling assimilating additional SYNOP data (blue) and the corresponding reference run (red). All forecasts were initialized at 0 UTC in April 2025.

Extended use of National SYNOPs from OPLACE at ALADIN/CZ

Martin Imrišek and Alena Trojáková (CZ) focused on newly available national synoptic OPLACE data from Croatia, Slovenia, and Slovakia. The quality of all available synoptic data was revalidated over a two-month period. New criteria were established to blacklist stations that either exhibited poor quality or were unrepresentative for the ALADIN/CZ configuration. The rejection quality criteria are listed in the table below.

Because the Croatian national and Bulgarian GTS data showed a significant bias in OMG—likely caused by incorrect metadata or poor measurement practices—the blacklisting criteria for these stations were made stricter to avoid assimilation issues. The new data and updated blacklist have been operational since the beginning of September 2026.

Table 1: Rejection criteria

	T2m [C]	RH2m [%]	U,V [m/s]	Geopotential [m^2/s^2]
Gross error = OMG >	15	80	15	200
Bias (OMG) >	1.5	30	1	100 but 20 for BU, HR stations
Stde (OMG)>	2.5	50	3	200 but 50 for BU, HR stations

High-resolution crowd-sourced surface observations (surface pressure, T2m, Q2m, V10m): further explore the potential of volunteered observations from crowd-sourced/private weather stations, cars, and smartphones (DA1.3).

No work reported.

Aircraft-based observations: assist implementation of Mode-S wind and temperature (EHS and MRAR); assess performance of fast observations from EMADDC. (DA1.4)

Experiments with EMADDC Mode-S EHS and MRAR data in AROME/HU data assimilation (including a 2-week visit at Météo France in July-August)

EHS pre-thinning bug fix: Siebren de Haan's preprocessing script contains a parameter that determines how much data can be loaded from a BUFR file. When this value is set too low, the script may fail to read the complete file. Due to the high density of Mode-S EHS observations, this can result in only a small fraction of the data being loaded, typically from the first few minutes of the one-hour processing window. To resolve this issue, Péter Elek (HU) leveraged the existing ecCodes library already integrated into the script. The new implementation uses ecCodes to determine the required BUFR message size before loading the data, ensuring that the entire message is read correctly. A simple workaround would have been to increase the buffer size to accommodate all possible BUFR files. However, this approach would unnecessarily increase memory consumption and execution time. The implemented solution avoids these drawbacks while ensuring complete data ingestion. Because previous thinning experiments may have been performed on incomplete datasets, the thinning parameters should be revisited and re-evaluated using the corrected preprocessing workflow.

Verification to EHS data: The forecast verification project, which compares forecast model output against aircraft Mode-S EHS observations, has been implemented and successfully tested internally (Figure 3). During development by **Péter Elek (HU)**, a significant memory-management issue was identified in the underlying ecCodes library which affected the processing workflow. The issue could cause the application to halt or crash during extended processing and, importantly, prevent reliable use of the originally planned parallel-processing approach. The stability and memory-related problems affecting normal operation have been resolved. However, the underlying constraints make efficient multi-node parallelization substantially more difficult to implement. The project is currently undergoing testing (by Benedikt Strajnar(SI)), and feedback is being collected to improve the overall user experience. The next development priorities are to incorporate tester feedback, simplify installation and deployment where possible, improve usability (including scaling) and documentation, and evaluate practical options for scalable parallel processing.

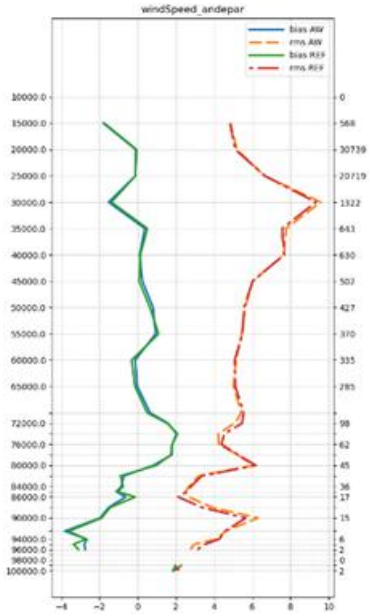


Figure 3: Example figure: two experiments with AROME (reference run and with adaptive weighting in cy46) verified against Mode-S EHS data for 1 selected day.

Preparation of whitelist for EMADDC EHS data (stay at Météo-France from 27 July to 7 August): The Mode-S EHS data assimilation with adaptive weighting had already been back-phased from CY49 to CY46 by **Péter Elek (HU)** and Vivien Pourret (FR), with preliminary preparations for introducing a whitelist. During my stay, we completed and tested the whitelist implementation in CY46. Following successful validation, I gained a thorough understanding of both the methodology and rationale behind the whitelist generation process (Figure 4). Building on this knowledge and the existing R implementation, I developed a Python version to improve integration and maintain consistency across our internal Mode-S software tools. We also revisited the topics of thinning and error correlation, although the same Desroziers method is already implemented in our system. I familiarized myself with the Météo-France R scripts and, after the visit, began comparing them with our existing Python implementation to identify any methodological differences and ensure consistency.

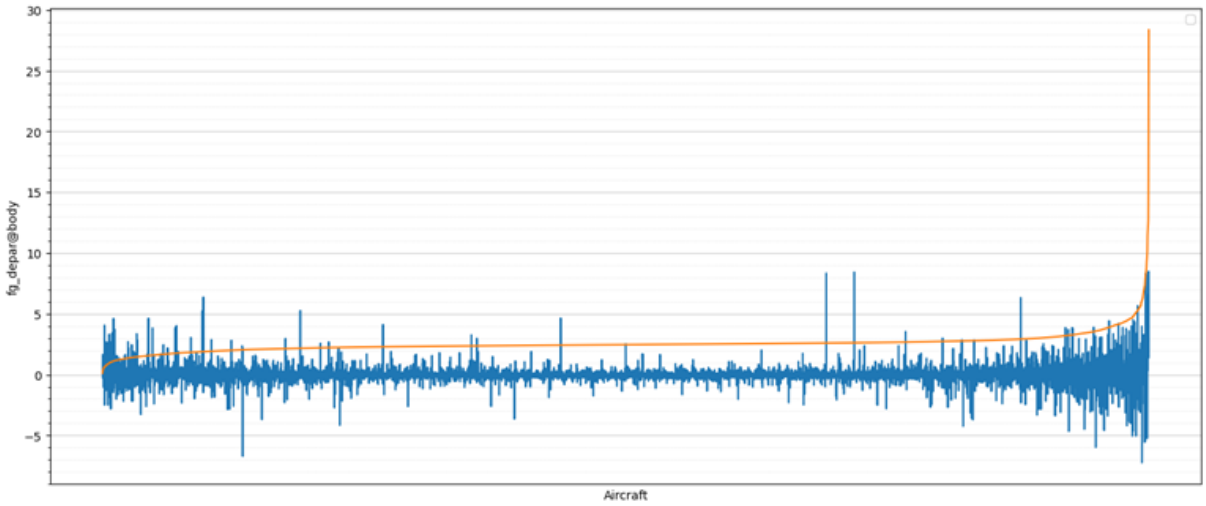


Figure 4: Aircraft first-guess departure statistics, ordered by standard deviation. Based on these statistics, we can identify aircraft with an excessively high standard deviation and determine that they are not suitable for inclusion on the whitelist.

Testing EMADDC MRAR data in AROME/HU: **Anikó Kardos-Várkonyi (HU)** started testing EMADDC MRAR data in AROME/HU at 2.5kmL60 with a 3-hourly assimilation cycle. The OPLACE was upgraded on 25 March 2026 to include EMADDC EU and FAST MRAR data, and began archiving these data for testing purposes. We performed an experiment from 1 to 7 April in order to check that the technical implementation of MRAR data into the data assimilation system was successful, and to verify the number of observations. In this experiment, we used the MRAR data without creating a dedicated blacklist for them, the experiment was carried out based on the current operational settings (used for AMDAR). Most of the data were added at the 12 UTC initialization (Figure 5), but some of these were removed during the thinning process. During this one-week period, no MRAR data were included in the 00 UTC and 18 UTC initialisations.

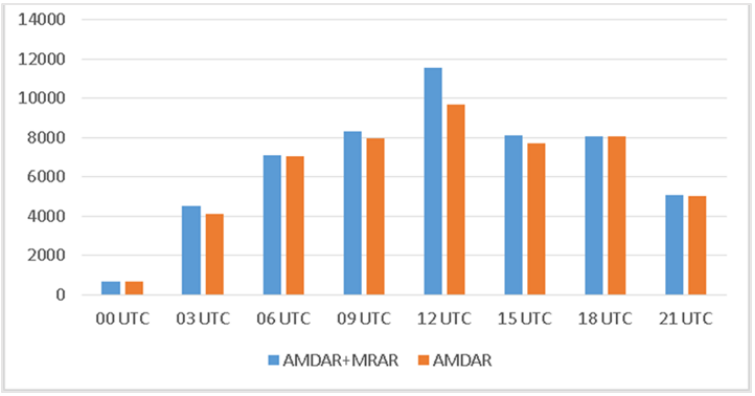


Figure 5: The number of AMDAR reports (orange), and the combined number of AMDAR and MRAR reports (blue) used in AROME/HU data assimilation between 1 and 7 April 2026 at different analysis time.

Creation of a common suite using MRAR and EHS data: A common assimilation suite has been created that integrates both EMADDC Mode-S EHS and Mode-S MRAR data. With this suite **Anikó Kardos-Várkonyi and Péter Elek (HU)** ran a 2-month experiment to support the creation of data selection rules and quality control within the data assimilation process (black and whitelists and the revision of thinning parameters). The next step is to check the impact on forecast performance using the newly created whitelist and blacklist. (2.75 PM)

Total efforts: 10.5 months

Contributors: P. Elek (HU) 2.25, A. Varkonyi (HU) 2.25, M. Nestiak (SK) 1, M. Imrisek (CZ) 4PM, A. Trojakova (CZ) 1PM

Documentation: /

Status: ONGOING

Subject: ***Use of ground-based remote sensing [DA 2]***

Description of tasks:

Implementation of reflectivity data assimilation (OPERA data) based on common preprocessing HOOF and benefiting from recent recommendations on tuning of Bayesian inversion (DA 2.1)

Setting up radar reflectivity experiment in AROME/HU data assimilation

Laura Magyar (HU) have completed and evaluated the optimization of the thinning parameters for AROME/HU at 2.5 km resolution. Four 1-month experiments were conducted during the summer period (04.07.–04.08.2025) to optimize the filtering parameters of reflectivity data using all five Hungarian radars. The namelist settings were selected based on the experiments performed with the ALARO/CZ model during the ACCORD/LACE stay in November 2025, as summarized in Table 2.

Table 2: Thinning configurations used for the AROME/HU experiments.

AROME_RADAR	thin1km	thin10km	thin20km	BatorSampling15km
HODIM%Sample	5000	5000	5000	15000
RMIND_RADAR	1000	10000	20000	16275
RFIND_RADAR	1000	10000	20000	16275
XYSHIFT_THIBOX(13)	0	0.5	0.5	0.5

For the treatment of “undetected” reflectivity data in the assimilation, the operational settings used at CHMI were applied uniformly in all experiments: RRADAR_OFFSET_DOE = 0.35 (in BATOR); RRADAR_RAINTHR = 0 (in Screening). The number of defined model profiles required for the Bayesian inversion was kept at the value used by the LACE countries (and Météo-France): NOBSPROFS(13) = 225. The first verification results indicated that the impact of the filtering settings was largest during

the period of the day with the highest precipitation occurrence (between 13 and 17 UTC). As shown in Figure 6 and 7, an increase in RMSE and bias values was observed during the first forecast hours of the 12 UTC cycles compared to the reference.

The correlation of observation errors in the AROME/HU radar experiment was examined using the ObsTool program written in R by Patrik Benáček (CHMI). The resulting correlation values were found to be more robust for AROME/HU than for the ALARO/CZ experiment and their convergence toward the 0.2 threshold defined by Liu and Rabier (2003) was considerably slower. This was presumably caused by the significantly (approximately ten times) smaller amount of data. When only the five Hungarian radars were assimilated, almost no reflectivity data entered CCMA above 400 hPa (and practically none above 300 hPa). The histograms of minimum distances between observations showed a distribution similar to that obtained in the ALARO/CZ experiments. The verification of the five radar experiments further indicated that the 15 km sampling distance provided the most favourable results for optimizing the filtering parameters. Consequently, the settings of the BatorSampling15km experiment were retained for the next simulations with all 26 radars covering the model domain.

Three 1-month experiments were carried out for the same period, assimilating all 26 radars to investigate the impact of the SIGMAO_COEF(13) (in BATOR) and LRADAR_NMBDO (in Screening) namelist parameters. The model set containing the MDRF code modifications provided by Antonín Bučánek (modset_batorCY46t1as_op1) was successfully integrated. Screening and minimization were executed on 2 nodes with 24 CPUs, while BATOR continued to run on 1 node with 48 CPUs. The evaluation of the results is currently ongoing.

As a follow up to the update announced on the ACCORD wiki (RD2) regarding the new OPERA release of 23 June 2026, we verified whether the preprocessing chain still functions correctly with the updated radar files. We found that the Polish files continue to contain only an empty TOTAL QC field, whereas the Czech files now include the /how/group with the NI attribute.

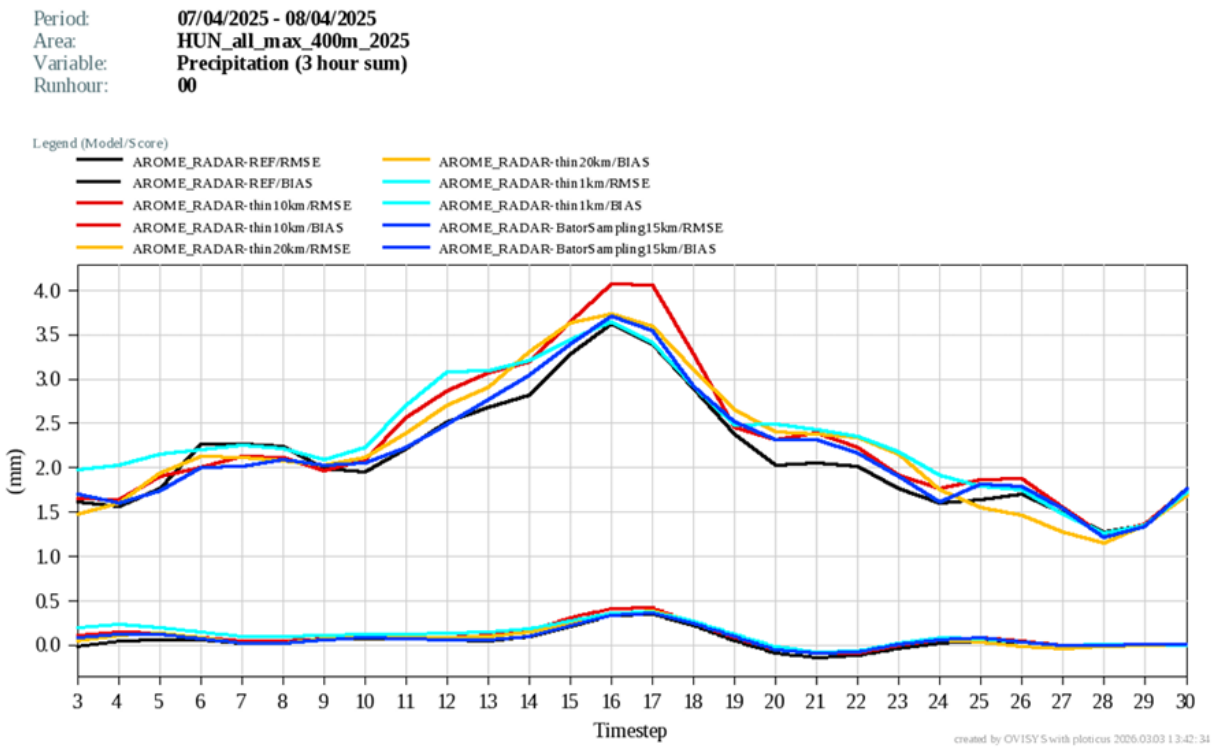


Figure 6: RMSE and bias of 3 hour precipitation forecast in function of lead time [h] for different AROME experiments, all initialized at 0 UTC from 4 July to 4 August 2025.

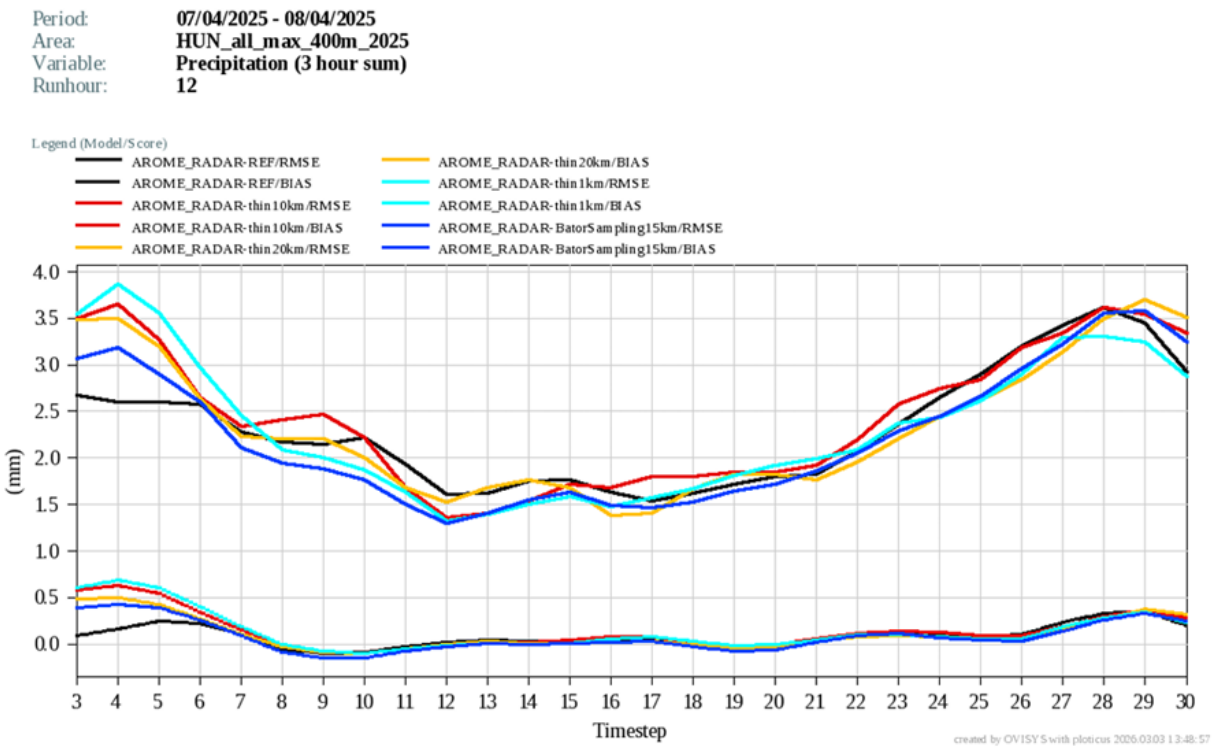


Figure 7: The same as Figure 1, just for runs initialized at 12 UTC.

Radar reflectivity assimilation in the 1-km SHMÚ ALARO-1 RUC [ALA1 - RUC1]

Michal Nestiak (SK), our ALA1 radar data assimilation testing suite runs every 6 hours at the main synoptic terms (00, 06, 12, and 18 UTC) with a 7-hour forecast on the same domain as our rapid update cycle (RUC1), due to limited computational capacity. The migration to cycle 48t3 is in progress.

Supercellural Cases: 20-21 August 2026, 18 UTC: Two supercells hit the Slovak territory on consecutive days: on 20 August at 15 UTC in the Bratislava region, and on 21 August at 21 UTC in the Rimavská Sobota region. Fortunately, only property damage was reported. To study these cases, we are gradually building analysis tools.

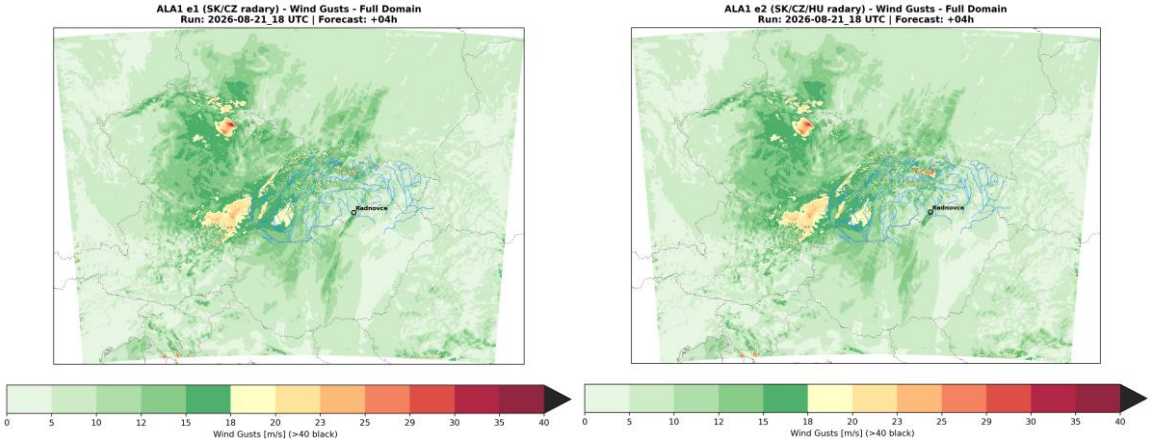


Figure 8: Comparison of simulated wind gusts between two experiments. Left: ALA1_e1 assimilating SK and CZ radars. Right: ALA1_e2 with added hubud radar to SK and CZ ones. The ALA1_e2 configuration yields stronger wind gusts, matching the observed reality more closely.

To decide which radar has better visibility for the studied region, we prepared a program that evaluates the best visibility from OPERA radars. It also calculates the minimum visible height, the minimum height of the radar ray, and the visibility layer height BASE 500-1000m.

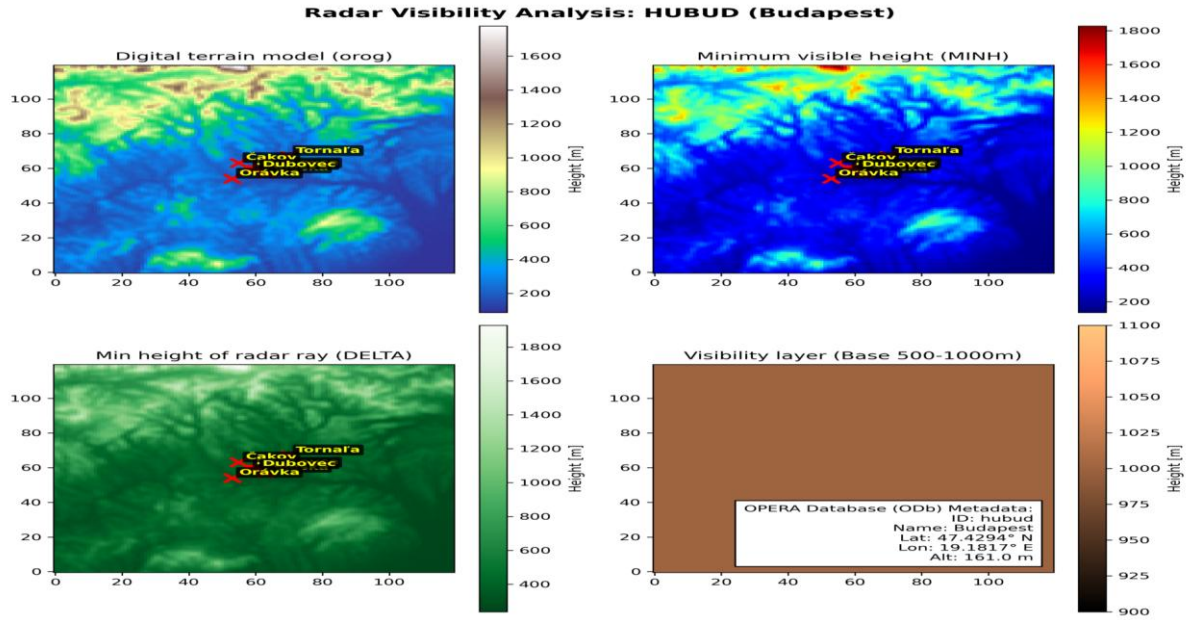


Figure 9: Radar visibility analysis for HUBUD radar.

Some radar related activity at Geosphere

Florian Meier (AT) developed a tool (python+epygram or Fortran binary in model code) to add hydrometeors to EPS members or first guess in case there are none. This is especially interesting in case of direct reflectivity assimilation within EnVar or could be also used within satellite all sky assimilation to define hydrometeor correlations in case they are not already in EPS for extended control variable. Part of humidity is converted to hydrometeors and temperature adjusted such that virtual temperature remains unchanged. Some tests were done during the LACE stay of Laura Magyar in August in Vienna. Furthermore, radar volume data from Italy in ODIM format were found on open data servers of ARPA Piemonte and Lombardia 2 x 2 stations in north Western Italy. We currently archive the data and will try to pre-process them for RADAR DA application.

Impact studies with original and de-aliased OPERA Doppler wind data. (DA 2.1)

Martin Petrovič (SK) carried out a three-week E-WFC Short Term Scientific Mission at CHMI Prague (26 April to 16 May 2026, host Alena Trojáková), focused on the assimilation of Doppler radar radial wind (DOW) observations from the EUMETNET OPERA network into ALADIN Cy48t3mas_op1 (2.3 km, 87 levels, 3-hour Blendvar assimilation cycle) over the ALADIN/CHMI operational domain. ODIM HDF5 volume data from the NIMBUS production line were homogenised with HOOF2.2.py (format conversion, harmonisation of Nyquist velocity, gain/offset), optionally dealiased with the torus mapping algorithm (Smerkol et al., 2025) and optionally converted into superobservations (SO). BATOR preprocessing used the wind cleaner, spatial median filter, background check and thinning (Sample=5000, Resolution=1000 m). A new namelist variable RZFACT was introduced to control the background-check rejection limit.

Six experiments were carried out for March 2026 in a "pivot" design, where each pair of configurations differs by exactly one degree of freedom:

- **r01 (Passive Reference)**: A passive control run encompassing the full network (77 radars

across 11 countries over a six-week period).

- **r02 (Active Baseline)**: An active three-country setup (FR, DE, and SK with 43 radars) with velocity dealiasing switched OFF.
- **r03 (Full Network)**: The complete radar network configuration with velocity dealiasing switched ON.
- **r04 (Dealiasing Test)**: Identical to r02, but with velocity dealiasing switched ON.
- **r05 (Tight Rejection Limit)**: Identical to r02, but applying a stricter rejection threshold (RZFACT=0.16, reducing the limit to ±8 m/s instead of the default ±17 m/s).
- **r06 (Filtering Test)**: Identical to r02, but utilizing superobservations and having the BATOR filtering switched OFF.

Data quality was assessed with a Block Bootstrap Anderson-Darling (BBAD) normality test (1000 observations resampled in contiguous 10-point blocks, 100 repetitions, median AD statistic), complemented by skewness, kurtosis and R^2. The quality dashboard was applied per radar, per elevation angle and per distance range. Forecast impact was verified against the operational CHMI suite.

The three-country baseline r02 showed an anomalous BBAD pattern in which the actively assimilated subset scored worse than the full dataset, with a raw innovation range extending to ±70 m/s, i.e. undealiased observations were passing the background check undetected. Dealiasing alone (r02 vs r04) reduced the raw innovation standard deviation from 4.333 to 3.692 m/s (−14.8 %), removed the anomaly and reduced RMS departures for DOW by roughly 7.5 % (OMA) and 8.5 % (OMG). The full 77-station, 11-country network (r03) gave the best active-subset quality (BBAD 0.1243, standard deviation 3.881 m/s). The tight rejection limit (r05) cut DOW RMS departures by −17 % (OMA) and −35 % (OMG), but this is a mechanical consequence of the truncation, since all other observation types remain unchanged. Superobservations without BATOR filtering (r06) produced a correct BBAD pattern for the active subset (0.1358) but a wider raw spread (4.781 m/s) and a clear inflation of RMS errors for surface-based observation types (SYNOP, RADAR DOW).

None of the six configurations produced a clearly positive forecast impact over the two-week evaluation period; the least negative were r04 and r03. A persistent positive bias (defined here as observation minus first guess) of about +0.2 m/s appeared in all experiments regardless of network configuration, dealiasing status or filtering method. Dealiasing is therefore a necessary but not sufficient condition for beneficial radar wind assimilation. A full report is currently being reviewed and will be available soon.

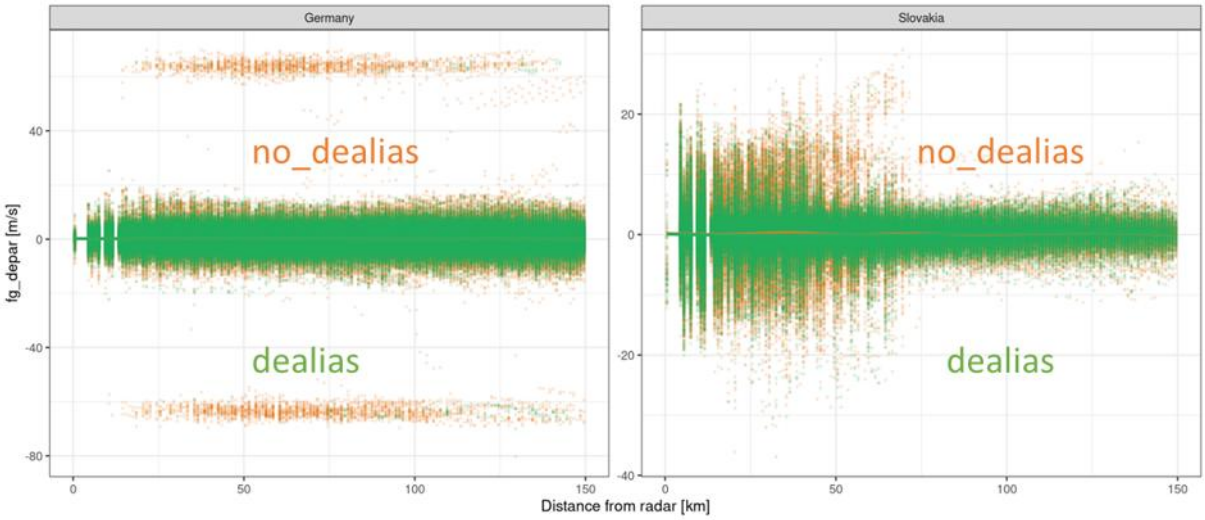


Figure 10: Scatter plot of first guess departures across distance for German radars (left) and Slovak radars (right) for experiment r02 (orange color – without dealiasing) and experiment r04 (green – with dealiasing algorithm).

Test of super observation functionality in HOOF for radar reflectivity (or alternatively radial wind). (DA 2.1)

No work reported.

Further elaborate the assimilation of GNSS ZTD observations and conduct impact studies, focusing on data from regional providers, assist quality improvement of solutions from these centers (DA 2.2)

Preparation of new GNSS ZTD whitelist for AROME/HU

The current whitelist was generated in June 2023, and some new networks have become available since then, including BMEL [Slovenia and Hungary (formerly known as SGO1)]. In addition, instead of numerous small ASCII files downloaded from the Met Office server, we now rely on a single BUFR data file obtained from OPLACE. Considering all these, **Helga Kolláthné Tóth (HU)** started to prepare a new whitelist. Passive assimilation was conducted from 1 to 28 February, 2026 (spin-up from 20 January), including ECMA ODB collection and whitelist generation from first guess departures using Paul Poli's program. The updated whitelist contains 145 stations from 12 networks, compared with 115 stations from 4 networks in the previous version. During the process, a bug was identified in the original program: pairs of nearby stations were both rejected instead of retaining one of them. After correcting this issue, the final whitelist contains 159 stations (Figure 11).

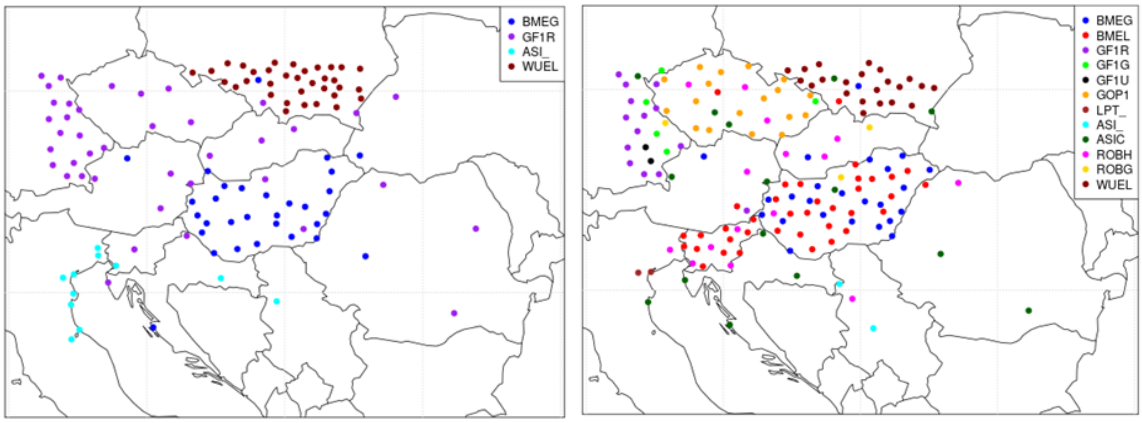


Figure 11: Selected stations and networks in the old (left) and new (right) whitelists for GNSS ZTD.

An experimental run was performed for March 2026 using the new whitelist (spin-up from 14 February). A 3-hourly data assimilation cycle was used and 30-hour forecasts were achieved at 0 UTC. The weather in this month was dominated by anticyclonic (generally calm) conditions, followed by a more unsettled and wetter period starting from 26 March onwards. Neutral results were obtained for 2 m temperature, while the forecast accuracy improved for relative humidity during the night and reduced during the day (Figure 12). The work will be continued by checking the impact in our high-resolution, hourly cycled AROME-RUC system.

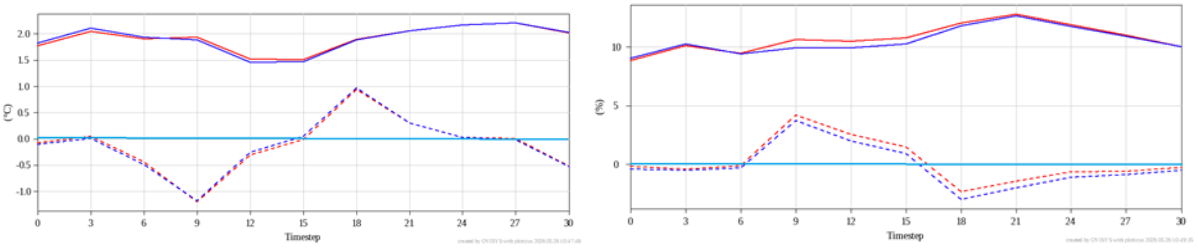


Figure 12: Bias (dashed) and RMSE (solid) of 2-metre temperature (left) and relative humidity (right) forecast in function of lead time [h] for AROME experiments using the old (blue) and the new (red) whitelist for GNSS ZTD data, all initialized at 0 UTC for March 2026.

GNSS slant delay impact studies with 3D-Var (DA 2.2)

No work reported.

Total efforts: 9.25 months

Contributors: F. Meier (AT) 1, M. Nestiak (SK) 1, A. Trojakova (CZ) 0.5, M. Petrovič (SK) 1, M. Imrišek (SK) 0.5, L. Magyar (HU) 4.25, H. Toth (HU) 1

Documentation: /

Status: ONGOING

Subject: *Satellite-based remote sensing observations [DA 3]*

Assimilation of clear sky radiances (DA 3.1)

Jachym Sevcik (CZ) and **Alena Trojakova (CZ)** investigated the use of microwave sensors (AMSU-A,MHS) onboard Metop-B/C in ALARO/CZ. Preparatory experiments assimilating the AMSU-A/MHS radiances in passive mode have been run to warm up the variational bias correction coefficients (VarBC). The VarBC warm-up did not converge for the low- and middle-peaking AMSU-A/Metop-C channels due to the smaller number of observations that passed the thinning and screening procedures. We identified a larger noise on AMSU-A/Metop-C ch4 as the cause, see the figures below for an illustration. Firstly, the innovations of ch4 are typically used as the primary thinning criterion, which leads to the prioritisation of AMSU-A Metop-B measurements over Metop-C measurements. This issue was addressed by proposing an alternative thinning approach that prioritises observations acquired closer to the model analysis time. Secondly, the first-guess departures of ch4 are used for cloud detection, resulting in an overly strict screening procedure for AMSU-A/Metop-C. This issue was addressed by running a second iteration of the VarBC warm-up for AMSU-A/Metop-C. Nevertheless, observation counts from this sensor remain low. Additionally, another cloud screening proxy, ch15, was found to be broken on AMSU-A/Metop-B, which disabled the use of its low and mixed channels. These findings complicate the assimilation of low-peaking AMSU-A measurements. The VarBC and MHS thinning/screening were found to be working well. Experiments involving active data assimilation with the AMSU-A high-peaking channels (9–12) and the MHS channels (including the low-peaking channel 5, with the dynamic emissivity method enabled) are ongoing.

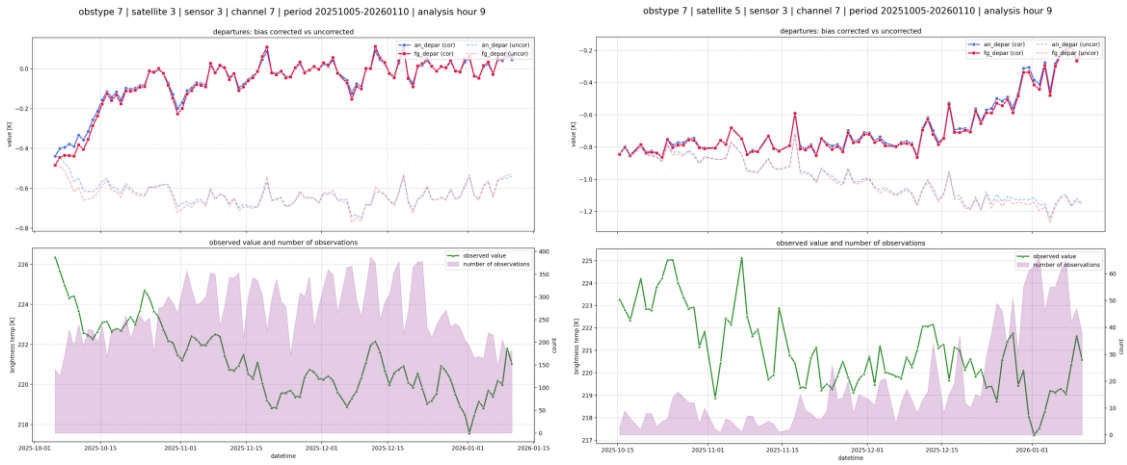


Figure 13: Time series of corrected and uncorrected first guess departures (top), number of observation counts and the mean obsvalue (bottom) for ch7 of AMSU-A Metop-B (left) and Metop-C (right).

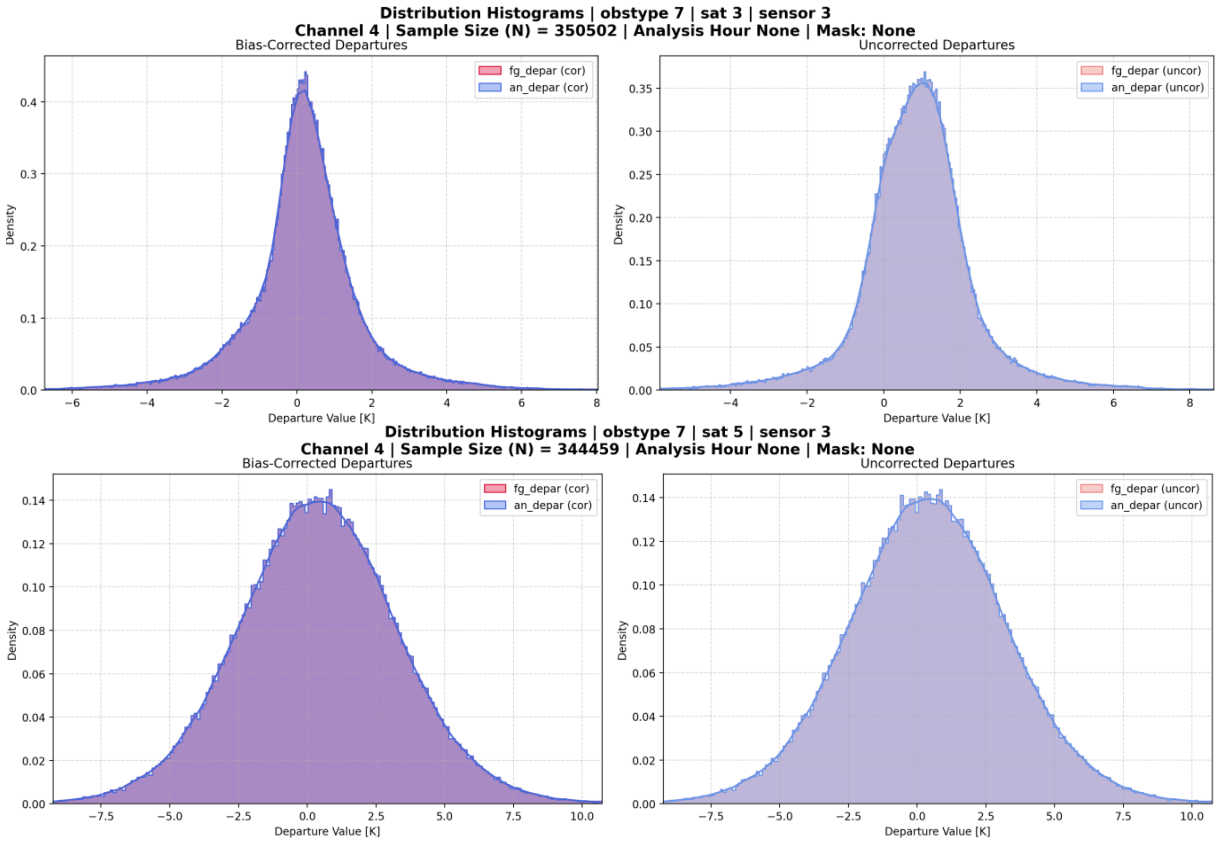


Figure 14: Histograms of bias-corrected (left) and un-corrected (right) first guess departures for AMSU-A ch4 from Metop-B (top) and Metop-C (bottom).

Assimilation of Allsky radiances (DA 3.2)

Florian Meier (AT) and **Adhithiyan Neduncheran (AT)**: All-sky assimilation of MTG FCI water vapor channels has been implemented and tested within the CLAEF-AlpeAdria AROME CY48T3 framework using a 3D-EnVar configuration, including ice particles in the control vector. Several case studies were conducted to assess the impact of assimilating MTG FCI observations under all-sky conditions.

Preliminary results indicate that all-sky assimilation of MTG FCI provides a modest but consistent improvement compared with MSG SEVIRI all-sky assimilation, particularly for forecasts of convective precipitation. Figure 15 shows a representative case in which the MTG FCI experiment achieved slightly improved precipitation skill scores and a better spatial representation of precipitation relative to the SEVIRI experiment.

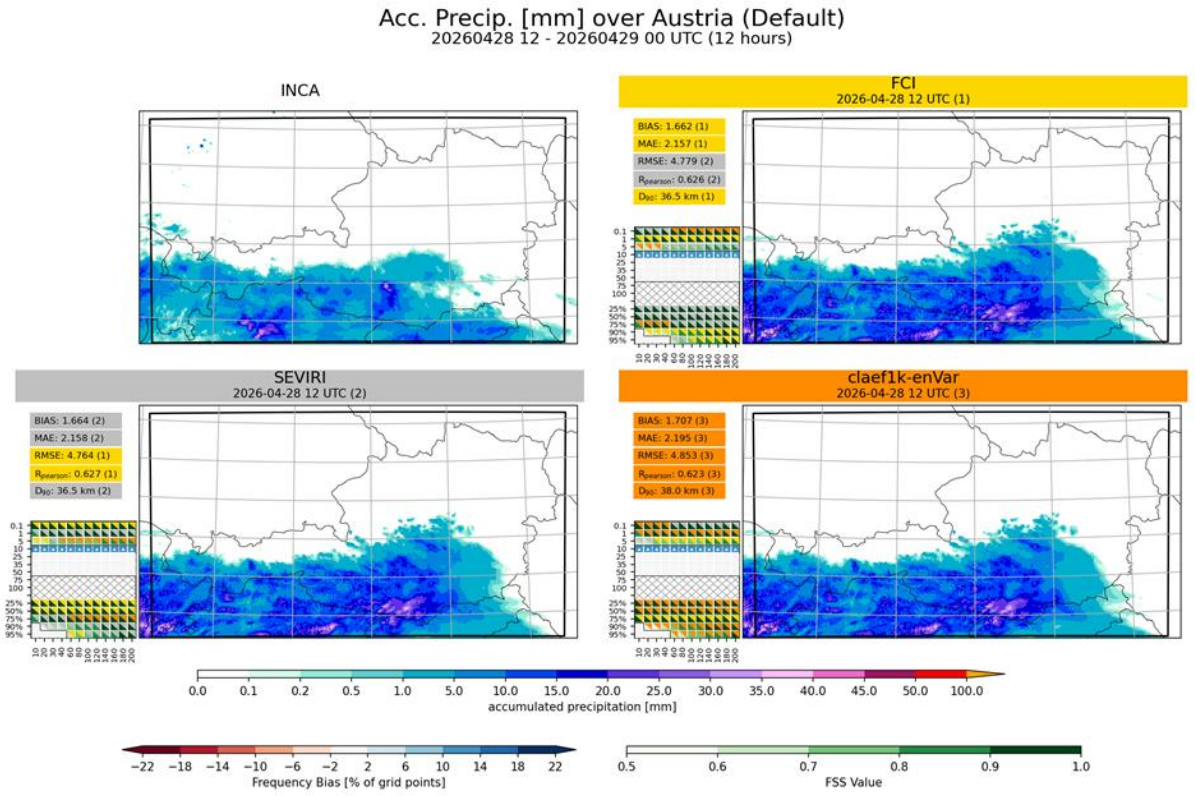


Figure 15: Verification of 12-hour accumulated precipitation forecasts over Austria. The CLAEF 1 km 3D-EnVar experiment serves as the reference configuration, including all operationally assimilated observations. The SEVIRI and FCI experiments show the additional impact of assimilating MSG SEVIRI and MTG FCI observations, respectively.

A short-cycled assimilation experiment was completed in August 2026 and is currently under detailed evaluation. In addition, a month-long cycling experiment for Summer 2026 is planned to quantify the impact of all-sky versus clear-sky assimilation of MTG FCI observations over an extended period and across a broader range of weather situations.

Following routine monitoring of MTG FCI and MSG SEVIRI observation departures during June 2026, the observation error specification for MTG FCI was re-evaluated and retuned. Based on this analysis, a newly developed Segmented Linear Interpolation Method (SLIM) was introduced to dynamically assign observation errors for all-sky assimilation following the Okamoto approach. This method better captures the dependence of observation uncertainty on cloud amount and cloud type, enabling a more realistic treatment of cloud-affected radiances within the data assimilation system.

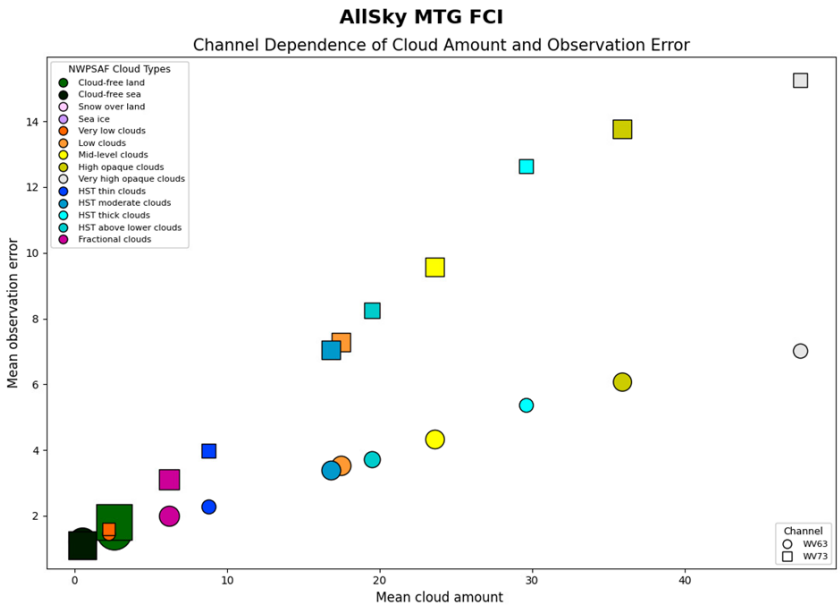


Figure 16: Dependence of observation error on cloud amount for MTG FCI water vapor channels (WV6.3 and WV7.3). Marker size is proportional to the relative number of assimilated observations associated with each cloud type.

As part of the development of visible-channel assimilation, a new switch, NFCIVIS(SATID), was introduced in bator, together with dedicated code modifications to separately ingest visible and infrared channels from different input files. This development is a prerequisite for the assimilation of MTG FCI visible channels, owing to their higher spatial resolution compared with the infrared channels. With this implementation, the system is now capable of handling visible and infrared observations independently, providing the necessary framework for future MTG FCI visible-channel assimilation experiments. In the absence of operational FCI visible test data, MSG SEVIRI visible-channel observations were used as a proxy to test and validate the approach within AROME CY48T3.

In parallel, work is ongoing to develop the interface for visible-channel assimilation using RTTOV-MFASIS-NN in AROME CY50T2, initially based on MSG SEVIRI visible channels. The objective is to establish a complete visible-channel all-sky assimilation capability and perform dedicated impact experiments during Summer 2027.

All-sky IASI data assimilation within the C-LAEF AlpeAdria

Suzana Panežić (CR) and **Benedikt Strajnar (SI)** continued their work on implementing the Okamoto method for all-sky IASI data assimilation within the C-LAEF AlpeAdria EnVar framework. With the development reaching the point of practical application, the AROME and MF ARPEGE code modifications were consolidated at the Helsinki DAWW and later accepted for the CY50T3 release.

During the code consolidation, a difference in how the two models handle poorly simulated RTTOV data was identified. The ARPEGE modification diagnosed poorly simulated data using a window channel, treating and rejecting the entire profile as overcast if Tb was below 230 K. Conversely, the AROME modification diagnosed data per individual all-sky channel, rejecting only channel 3105 data when Tb fell below 240 K (same limit was diagnosed from the window channel 1191) [Figure 17].

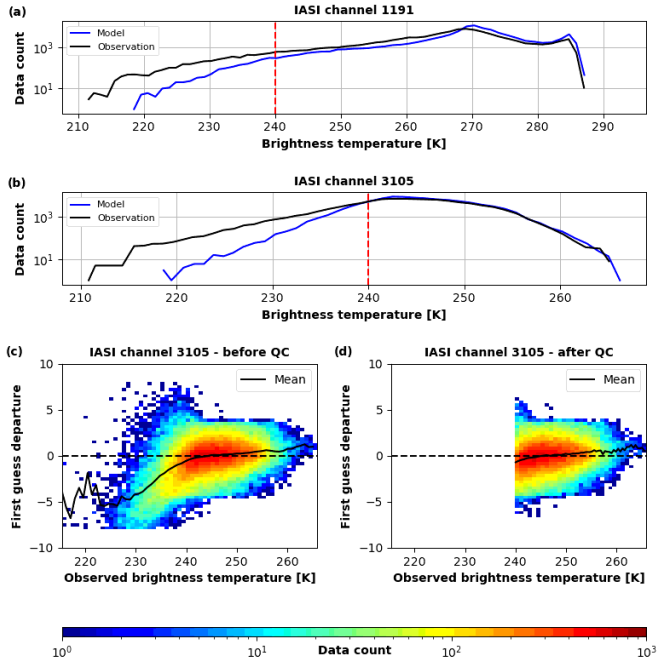


Figure 17: Comparison of observed and simulated brightness temperatures and first-guess departures for IASI channels. Data count versus brightness temperature for channels 1191 (a) and 3105 (b); the red dashed line marks the 240 K threshold. 2D histograms of first-guess departures versus observed brightness temperatures for channel 3105 before (c) and after (d) quality control (QC). Solid lines show binned means, and the bottom colorbar indicates data density counts on a log scale.

Both methods for rejection of poorly simulated data were used to mitigate the near-surface cooling and moistening causing the analysis degradation when compared to referent experiments with no IASI data assimilation. To investigate the underlying mechanism, single-observation experiments were performed using channel 3105 data with Tb < 240K and a large first-guess departure. To visualize the corresponding background error covariance structure, a Dirac test was conducted [Figure 18] by applying a unit impulse in control-variable space and propagating it through the square root of the **B**.

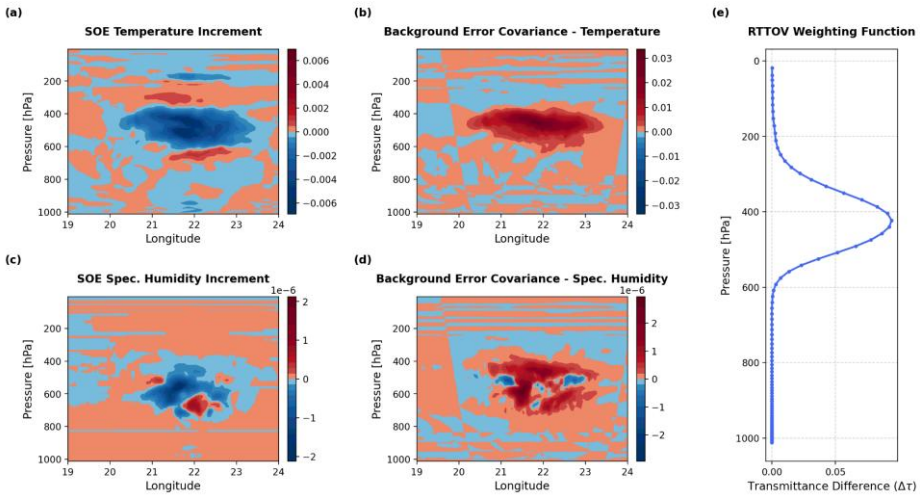


Figure 18: Single observation experiment temperature (a) and specific humidity (c) increments with corresponding background error covariances for temperature (b) and specific humidity (d), RTTOV weighting function (e) shown as transmittance differences between model levels.

The experiments revealed that neither the flow-dependent **B** in 3D-EnVar nor the operator weighting functions were sensitive to the surface, confirming that the overly broad vertical localization was not the cause. Instead, the degradation was found to originate from the VARBC thickness predictors, specifically the 1000–300 hPa predictor. During the minimization step, the bias correction was applied across this entire 1000–300 hPa column, demonstrating that the predictor is too wide and ill-suited for all-sky channels.

To evaluate the optimal quality control (QC) configuration, several experiments were conducted covering the period from January 15 to February 15, 2025 and verified against independent data (radiosonde and aircraft data). The baseline reference used an experiment that rejected only data with an averaged cloud effect below 5 K (Okamoto, 2023), designated as QC_CA5.

To evaluate methods for rejecting poorly simulated data, two distinct configurations were tested against this baseline:

- QC_CA5_TB1191: Incorporates the MF modification to reject entire overcast profiles.
- QC_CA5_TB3105: Applies the channel 3105-specific rejection method.

Additionally, two alternative approaches were analyzed to address the underlying degradation mechanisms:

- QC_CA5_noth: Retains the poorly simulated data but deactivates the VARBC thickness predictors.
- QC_CA5_E: Employs an extended control vector that includes cloud liquid water and cloud ice to determine if an improved model representation of hydrometeors mitigates the deficit in high ice clouds responsible for the large first-guess departures.

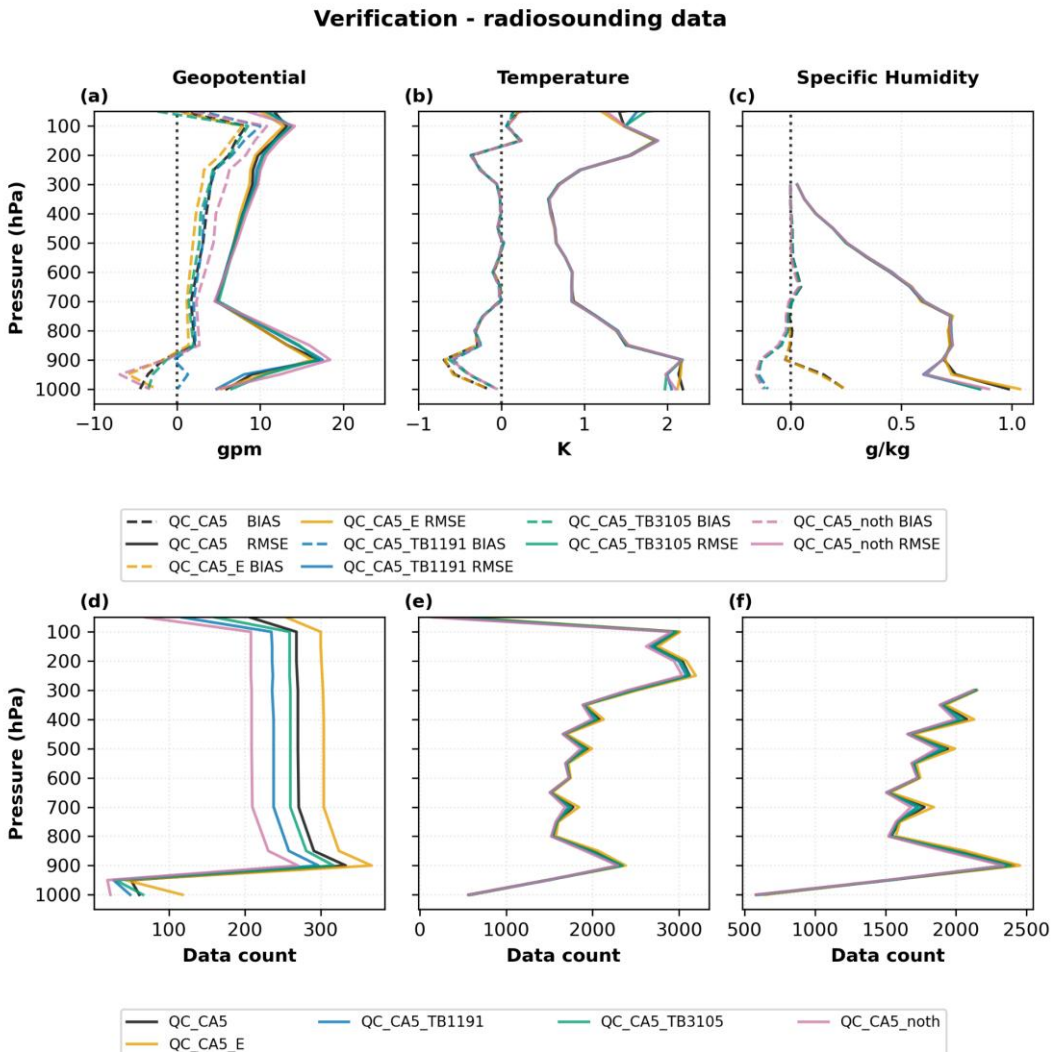


Figure 19: Verification of analysis against radiosonde observations during the period 15th January–15th February 2025. Bias and RMSE of (a) geopotential, (b) temperature, (c) specific humidity, and data count of (d) geopotential, (e) temperature, (f) specific humidity for the QC_CA5, QC_CA5_E, QC_CA5_TB1191, QC_CA5_TB3105 and QC_CA5_noth experiments.

The results showed that QC_CA5_TB1191, QC_CA5_TB3105, and QC_CA5_noth all successfully mitigated the near-surface cooling and moistening. Notably, QC_CA5_TB3105 retained the highest volume of radiosonde [Figure 3] and aircraft observations, implying a superior representation of the background state. On the other hand, while QC_CA5_E demonstrated no skill in mitigating the near-surface degradation, it retained the largest amount of independent data. This indicates that an improved model representation of hydrometeors holds the potential for broader long-term benefits.

The data assimilation system was tuned using ObsTool alongside modeled and diagnosed variance diagnostics to determine the optimal thinning distance and observation error inflation factor. For the clear-sky experiment, the optimal configuration yielded an 80 km thinning distance and an inflation factor of 2.0. In contrast, the all-sky experiment required a 60 km thinning distance and an inflation factor of 1.75.

Using these parameters, three experiments were performed covering the period from January 15 to February 15, 2025 and their forecast verified against over 1700 stations across Europe:

- REF0: A reference baseline run with no all-sky or clear-sky data assimilation.
- CLRS: The clear-sky configuration, thinning distance 80km and inflation factor 2.0
- ACTS: The all-sky configuration, utilizing the optimal QC_CA5_TB3105 quality control setup, Okamoto observation error model, thinning distance 60km and inflation factor 1.75

Results showed overall better scores for ACTS when compared with both REF0 and CLRS, with the most pronounced improvements observed in the moisture and cloud fields during the first 15 hours of the forecast [Figure 4].

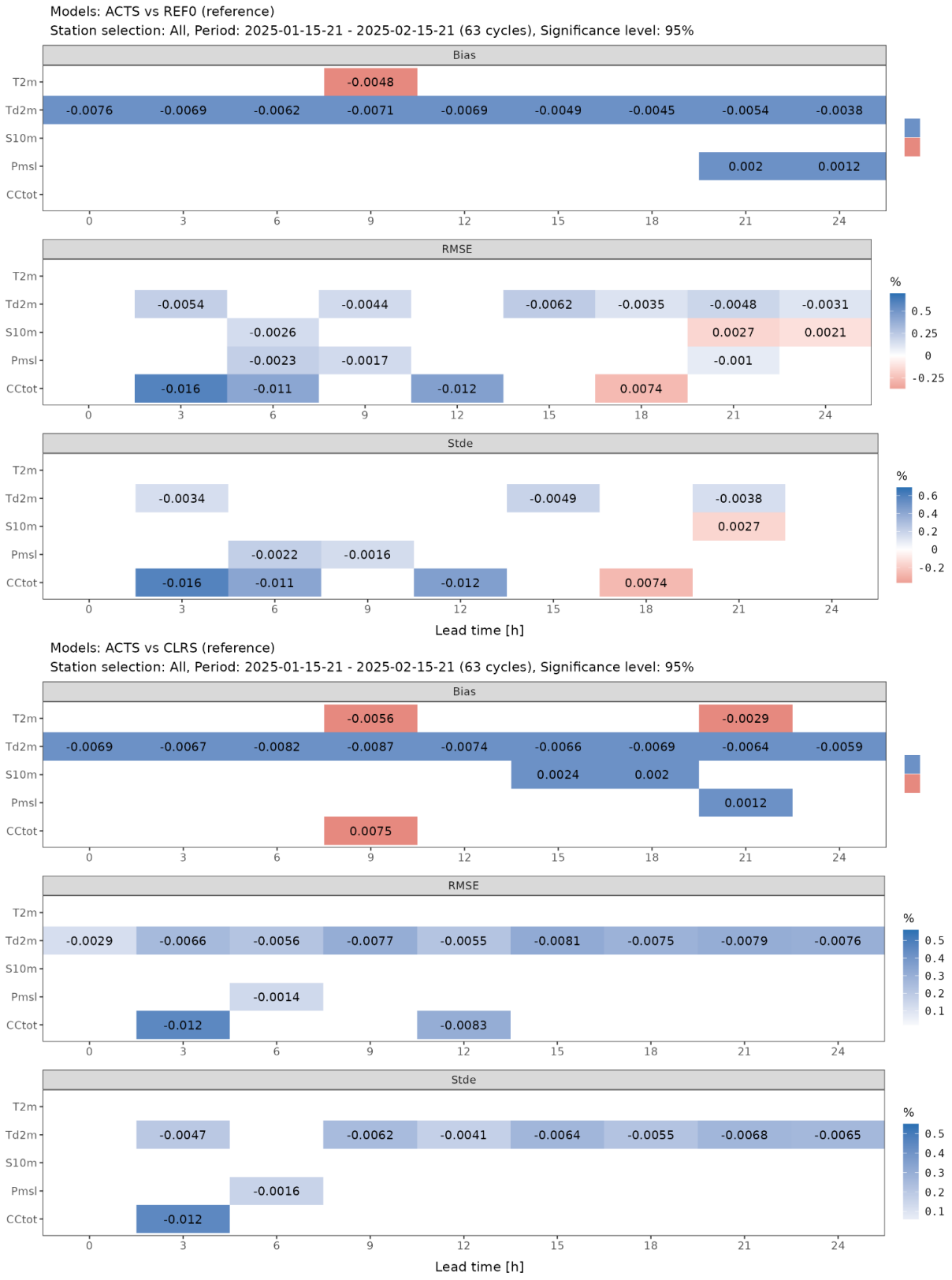


Figure 20: HARP scorecards for ACTS vs REF0 and ACTS vs CLRS experiments; blue color indicates ACTS experiment is better with the significance level of 95%; surface scores.

Atmospheric Motion Vectors (AMV). (DA 3.6)

Florian Meier (AT) tested MTG FCI geowind (bufr file from EUMETSAT) within AROME. Only very little adaptation (allow satellite ID 71 and set BATOR namelist accordingly, add bufr file to geowind bufr) was needed to let the observation pass through assimilation in cy43t2 and cy48t3. Increments look reasonable and data density is similar to SEVIRI-HR product. Also FCI-HR product (NWC-SAF bufr from local production line at Geosphere) was tested, but failed in BATOR as the file content differs from EUMETSAT's product. This needs further investigation.

Total efforts: 10 months

Contributors: F. Meier (AT) 0.25, A. Neduncheran (AT) 3.75, S. Panežić (HR) 2.5, B. Strajnar (SI) 0.75, J. Ševčík (CZ) 2.25, A. Trojáková (CZ) 0.5PM

Documentation: /

Status: ONGOING

Subject: *Observation pre-processing, quality control, bias correction and representation error [DA4]*

Benedikt Strajnar (SI) worked on the implementation of Slovenian GNSS observations into the OPLACE system.

Maintenance and development of ODB software and tools (DA 4.1)

No work reported.

Regular upgrades of the HOOF preprocessing tool. (DA 4.2)

No work reported.

Tuning of observations and background and representation error, revise thinning, QC and VarBC settings. (DA 4.5)

No work reported.

Information on OPLACE maintenance work and developments is provided in the DM's report.

Total efforts: 0 months

Contributors: A. Trojáková (CZ), Z. Kocsis (HU) see DM's report.

Documentation: /

Status: ONGOING

Subject: ***Variational assimilation systems [DA5]***

Develop, validate and consolidate full assimilation cycles using OOPS binaries (DA 5.1)

No work reported.

Maintenance, setting up and evolution of current DA suites (3D-Var, BlendVar), exchange of scientific achievements between ACCORD partners. (DA 5.6)

Poland is continuing preparatory works for 3D-Var assimilation setup, due to migration to new HPC works are delayed.

Large scale information in LAM (DA 5.7)

Maria Derkova (CZ), in collaboration with **Radmila Brozkova (CZ)**, investigated the blending by digital-filter (DF) setup in the ALADIN/CHMI BLENDVAR configuration. The work was motivated by cases of missing convective precipitation in the early hours of ALADIN forecasts, as reported by CHMI duty forecasters. The hypothesis was that this could be related to a dry humidity bias in the Arpège analysis (which is indicated by the verification scores) that may be introduced through DF blending. A series of experiments was therefore designed to investigate whether the current operational setup is optimal and how it could potentially be improved.

To recall, the operational ALADIN/CHMI data assimilation cycle is based on CANARI optimal interpolation for surface and soil parameters and the BLENDVAR algorithm, which consists of digital-filter (DF) blending followed by 3D-VAR analysis for the upper-air variables. An independent assimilation cycle is performed every three hours with a long cut-off time, providing the guess for the short cut-off production analysis and the subsequent forecast. At the intermediate synoptic network times (03, 09, 15, and 21 UTC), lagged Arpège lateral boundary data from the previous long cut-off assimilation step are used.

First, a simple approach was tested in which the blending of specific humidity was omitted either in both the assimilation and production analyses or only in the production analysis. In a second experiment, no blending was applied at the intermediate assimilation network times (NTs). These two approaches were then combined: no blending was performed at the intermediate synoptic NTs, and specific humidity was not blended in the production analysis. In addition, a configuration completely without blending was tested, with only 3D-VAR active for the upper-air variables. Finally, a configuration in which the order of the blending and CANARI steps was reversed was evaluated.

Table 3: List of experiments

EXP	**description**
ec0	reference for 48t3mas_op1
ALAD	real operational reference
ec1	no blending of qv in Assim and Prod
ec2	blending of qv in Assim, but no blending of qv in Prod
ed2	no DF blending at 03, 09, 15 and 21 UTC
ef1	no DF blending at 03|09|15|21 UTC and no blending of qv in Prod
ef4	no DF blending at all
eh3	swap canari and DF blending

The impact of the new configurations with respect to the reference setup was evaluated both through several case studies and in offline parallel suites. The case studies included selected convective precipitation events in July and August 2025, as well as the Boris storm case, which caused severe flooding in Central Europe in September 2024. The offline e-suites covered the convective season in July and August 2025, a short period of stable winter conditions in January 2026, a longer winter period in January 2026, and spring 2026.

Although omitting the blending of specific humidity appears to be beneficial for capturing the initiation of convective events (Figure 21), with a positive impact also seen in the precipitation verification scores, its impact on the verification scores in winter is sometimes detrimental. The experiment without blending performs worse compared to the reference for most of the verified parameters. Swapping the order of CANARI and blending steps also yields worse verification scores wrt the operational reference. The most promising configuration, considering both the verification scores and the benefits for the first forecast hours in convective situations, appears to be the one in which no blending is performed at the intermediate synoptic hours (Figure 22). However, this configuration needs to be reevaluated in the future operational version of ALADIN/CHMI currently under preparation, which will use a horizontal resolution of 1.25 km and the SURFEX scheme.

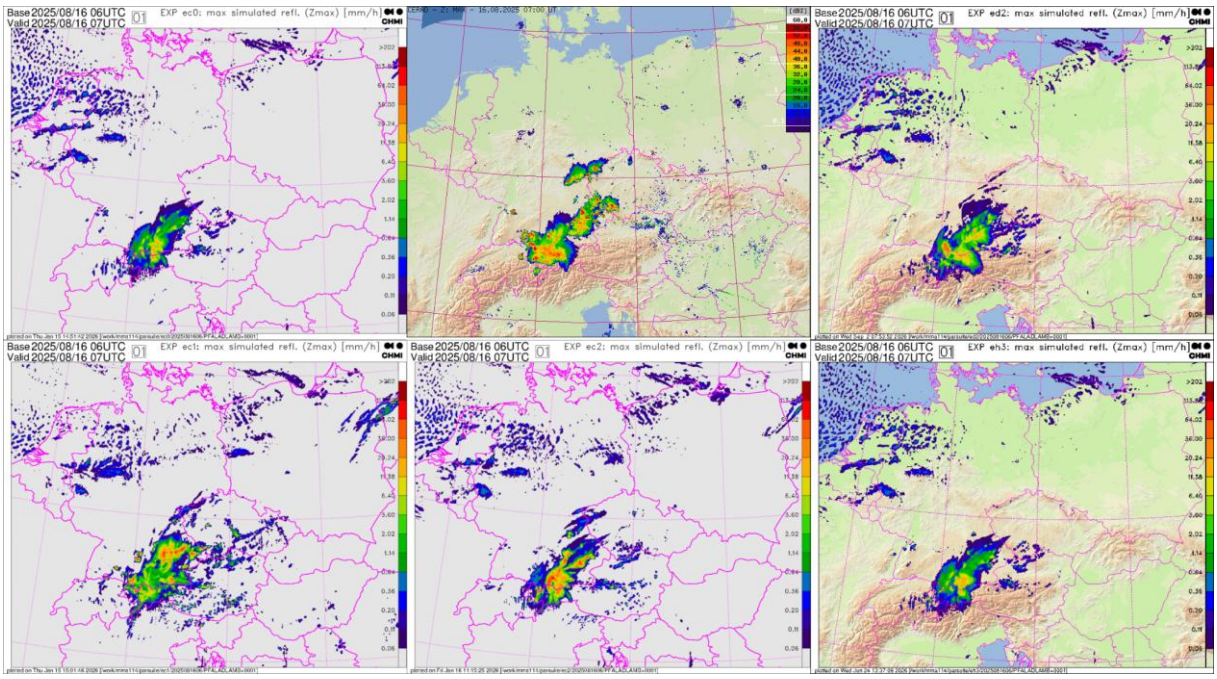


Figure 21: Case study for 16 Aug 2025 7 UTC - 1 h forecasts from 2025/08/16 06 UTC, a simulated maximum reflectivity field. From left to right and top to bottom: ec0 the reference forecast; the CERAD composite; ed2 the experiment with no blending at the intermediate synoptic hours; ec1 the experiment where no blending of specific humidity is applied both in assimilation and production; ec2 as ec1 but blending of q omitted only in production; eh3 the experiment with blending and canari steps swapped.

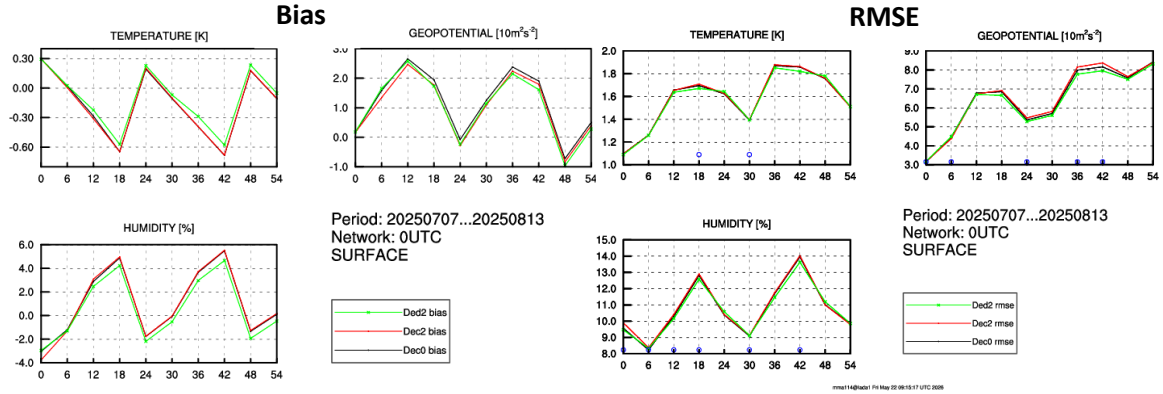


Figure 22: Bias (left) and RMSE (right) verification scores over summer period 2025 for the reference ec0 (black), ec2 exp. with no blending of spec. humidity in production (red) and ed2 exp. with no blending in the intermediate synoptic hours (green) for T2m, MSLP and relative humidity.

Total efforts: 5.5 months

Contributors: M. Derkova (CZ) 5, R. Brožková (CZ) 0.5

Documentation: /

Status: ONGOING

Subject: ***EnVar, EDA and variants [DA6]***

Prepare a prototype of full-scale OOPS-based 3D/4D EnVar system (DA 6.1, DA 6.2)

Florian Meier (AT) tested 3DEnVar with sub-ensembles in CY48t3bf3 (modset from Strajnar/Vogt) and added the option to have different inflation values (REDNMC equivalent namelist switch in EnVar) for the different sub-ensembles. In the case of C-LAEF_AlpeAdria setup, the impact on increments is clearly visible. However, the change in spread/error between the sub-ensembles (+3h and +6h forecasts from C-LAEF AA EDA) seems to be smaller than expected and therefore other modifications like change in horizontal localization length had more impact. It was also found by idealized studies at the University of Vienna that the currently applied low level localization length of 30km might be too small for the Austrian area (60km created better fit to observations in short range forecast).

Benedikt Strajnar (SI) investigated the performance of 3DEnVar wrt. 3DVar control in the operational ClaefAA runs. The classical verification over summer 2026 indicates a noticeable and consistent improvement in almost all surface variables, including variability and biases. Interestingly, after a lesser fit to observations at the analysis time, the differences may be seen for the whole forecast period, up to +60h. While precipitation is also significantly improved in 3DEnVar up to +6-12h into the forecast, the 3DVar control performed better (ETS and frequency bias) for thresholds above 25 mm/3h, both runs overestimating precipitation amounts in general. This is consistent with conclusions based on the panelification approach in certain high-precipitation events in summer 2026.

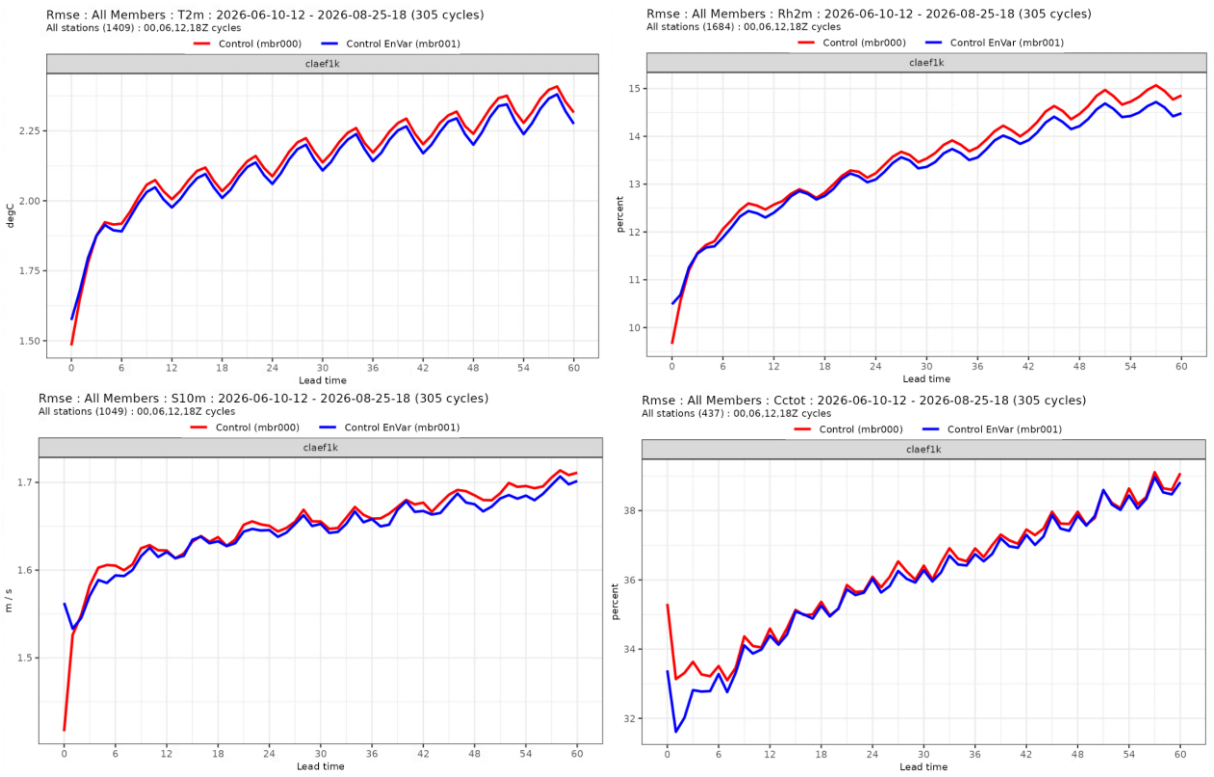


Figure 23: Comparison of 3DVar (red) and 3DEnVar (blue) controls runs in the ClaefAA ensemble over summer: RMSE evolution of 2m T, 2m RH, 10m wind speed, and cloudiness respectively.

Total efforts: 6.5 months

Contributors: F. Meier (AT) 3.5, B. Strajnar (SI) 1.25, A. Neduncheran (AT) 1.75

Documentation: /

Status: ONGOING

Subject: ***Initialization methods and nowcasting [DA7]***

No work reported.

Subject: ***Diagnostic methods, optimization of assimilation cycling [DA8]***

No work reported.

Subject: ***AI/ML methods for data assimilation [DA9]***

No work reported.

Subject: ***Surface assimilation [SU1]***

Implementation, experiments, design of parallel suites with OI and SYNOP observations in AROME or ALARO with SURFEX or ISBA. (SU1.1.11, SU1.2.1)

Development of SYNOP-based snow analysis in CANARI. (SU1.1.4)

The implementation of snow analysis for the ALARO CSC at CHMI using the ISBA scheme continued. Three configurations of the assimilation scheme were pre-selected:

- FR: inspired by Météo-France uses the Gaussian correlation function, default first-guess QC, no spatial QC, rejects any observation above 1500 m;
- AT-gauss: proposed by F. Meier uses the Gaussian correlation function, adapted height dependent first-guess QC, enables spatial QC, use data above 1500 m;
- AT-Mescan: proposed by F. Meier uses the adapted MESCAN correlation function, first-guess QC with height dependent σo, enables spatial QC, uses data above 1500 m.

The last two experiments aimed to use observations at high altitudes. A more benevolent QC was necessary to achieve this, and two alternatives were proposed. The specific tuning parameters (correlation length scales, observation and background errors, QC thresholds) of these three configurations were tuned using the Nelder–Mead simplex method for minimizing a tailored cost function. The results demonstrate a significant improvement in snow depth forecasting compared with both the reference without snow depth analysis and the default FR setting. The complete results of the study are to be summarised in a forthcoming article.

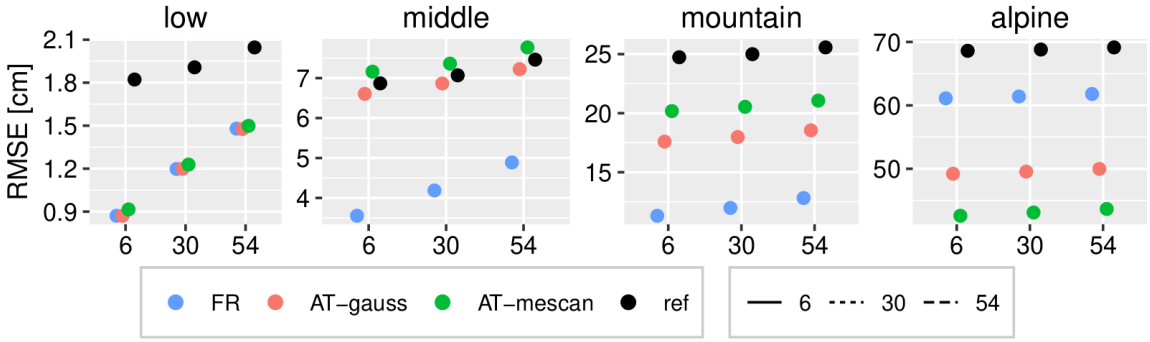


Figure 24: RMSE of snow depth as a function of forecast lead time for period of Jan 2022.

The AT-Gauss configuration has been selected for pre-operational testing, with development phased into model version CY48t3mas. The impact of the new assimilation scheme on other near-surface variables was mixed. Significant surface cooling was observed, affecting the screen-level temperature, with a degradation in its forecast for shorter ranges up to 18 hours and an improvement in the T2m forecast for longer lead times. The negative effects on the screen-level temperature and relative humidity were mitigated by adjusting the gridbox snow fraction (WCRIN). This quantity represents the proportion of the gridbox surface covered by snow, impacting both the resulting gridbox albedo and emissivity. The result of this retuning can be seen in Figure 2. The original experiment (AT-gauss) without any snow fraction modification results in lower screen-level temperatures than the snow-

analysis-free reference (black). The experiment with the retuned snow fraction (green) demonstrates the ability to mitigate the cooling effect, as it aligns with the reference BIAS, while maintaining the accuracy of the snow depth forecast.

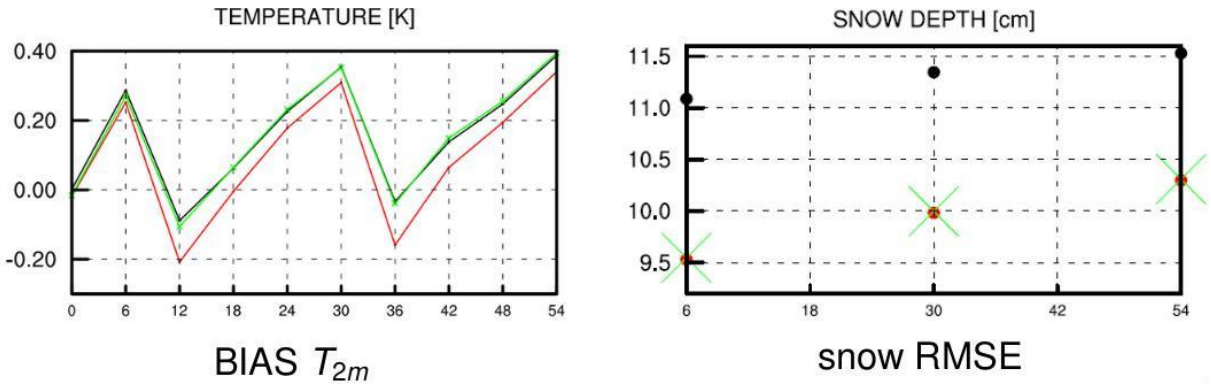


Figure 25: BIAS of screen level temperature and RMSE of snow depth forecasts, snow-analysis-free reference (black), the AT-gauss setting without (red) and with (green) retuned snow fraction.

This new snow depth assimilation scheme in the ALADIN/CHMI was implemented operationally on 1 May 2026. Work by **Jáchym Ševčík (CZ)** and **Alena Trojáková (CZ)**, with the support of **Florian Meier (AT)**.

New snow observations from Switzerland

Florian Meier (AT) found additional snow observations on Meteo Swiss open data hub. Those data (130 manual and 76 automatic at 06UTC) were converted into obsoul and fed into AROME-RUC. The data improves observation coverage especially in the Northern more flat part of Switzerland where SLF data are scarce.

2D-Var and 2D-EnVar evaluation and development (SU1.1.6)

Initial Evaluation of 2DEnVar for Screen-Level Data Assimilation in the Claef Alpe Adria Ensemble

Recent developments at Météo-France on the application of 2DEnVar to screen-level observations, including 2-metre temperature, 2-metre humidity, and land-surface temperature (LST), have shown promising results. We would like to investigate the feasibility of applying this approach within the Claef Alpe Adria (Claef AA) ensemble system. Sophie Marimbordes and Camille Birman have kindly provided the relevant code, which is based on the French CY48T1 OP1 configuration and implemented within the OOPS framework. This code has been successfully compiled on the ATOS system at ECMWF. The implementation also includes scale-dependent localization, which is potentially important for representing the spatially heterogeneous and terrain-dependent error structures relevant to screen-level observations.

A technical difference between the French configuration and Claef AA is that the French ensemble members and analysis use different domains, whereas Claef AA uses the same domain for both. The current implementation relies on FullPos routines for interpolation, which are problematic when the input and output domains are identical. For the initial test, whose primary purpose was to establish a

working reference configuration, we therefore generated a slightly smaller domain and first guess file using Tactus to avoid this issue. After some troubleshooting, we obtained a working 2DEnVar configuration. The resulting 2-meter temperature increments are shown in Figure 1. The increments are currently excessively localized around the observation locations, for reasons that are not yet understood. Changing the SDL parameters or inflation of background perturbations seem to only have a negligible effect regarding this problem, at least in our particular test case. Nevertheless, some terrain-dependent structures are visible in mountainous areas, which is qualitatively consistent with the flow-dependent background-error information expected from an ensemble system.

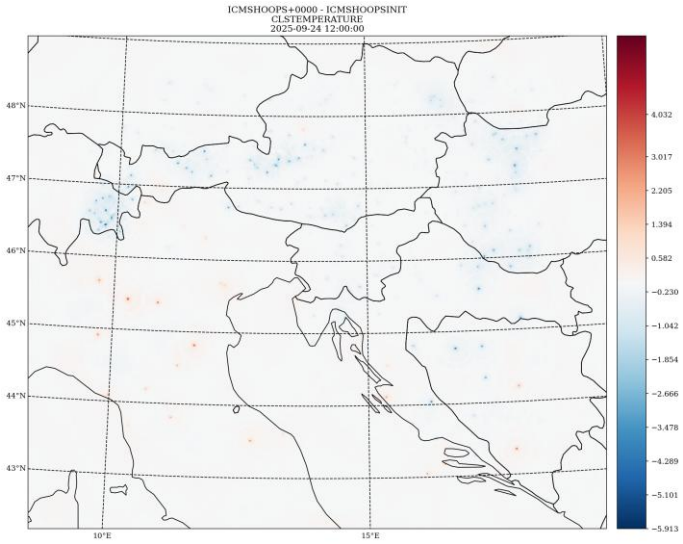


Figure 26: T2M Increments on a reduced Claef AA domain produced by an 2DEnVar analysis.

Before a proper experiment can be performed, the developments need to be ported to the CY48T3 IAL pack used by Claef AA for EnVar assimilation. Ideally, both EnVar and 2DEnVar should use the same executable, although this is not yet possible even in the French CY48T1 OP1 implementation. In addition, a version that avoids the FullPos interpolation step needs to be developed, which would allow the method to be applied directly on the full Claef AA domain. Reported by **Matjaž Ličar(SI)**.

Tuning of OI soil assimilation (SU1.2.1)

Initialization of SURFEX coupled with CANARI

Antonín Bučánek (CZ) was on a scientific stay at the Croatian Meteorological and Hydrological Service (DHMZ, Zagreb) in March 2026, focusing on the initialization of the SURFEX coupled with the ALARO using surface data assimilation. During the research stay, Antonín and **Anamarija Marjanović (HR)** identified and resolved the main technical hurdles and bugs obstructing the execution of the CANARI scheme with SURFEX (LAEICS_SX=T) on cycle 48t3. They achieved stable execution across different compiler platforms by fixing critical code issues, such as the uninitialized CSELECT variable and missing SST values for land-only MPI blocks. The outcome of the stay will be presented in the ACCORD newsletter.

Validation of ALARO with SURFEX using CANARI (1.25 km)

Radmila Brožková (CZ) carried out experiments to test the surface assimilation configuration using SURFEX and CANARI. The model domain covers Central Europe with a horizontal resolution of 1.25 km and 87 vertical levels. The atmospheric physics is based on ALARO, with minor adaptations for the high horizontal resolution. Within the assimilation cycle, only DFI blending with ARPEGE analysis is currently used, as the B-matrix is not yet ready. For reference, a baseline simulation was run with the same setup, but utilizing ISBA instead of SURFEX.

All basic experiments start cycling on 1st November (annual minimum of hydrological activity) of 2025. So far, several issues were found and fixed. Regarding the surface assimilation, care must be taken about packing SURFEX fields to sufficient precision. In addition, changes in SURFEX tuning interplay with the assimilation cycle. Work on this topic continues.

Assimilation of satellite moisture information (SWI) within SEKF in AROME/SURFEX, impact experiments (SU1.3.4)

No work reported.

Total efforts: 13 months

Contributors: M. Szczech (PL) (reported in DA5 ?pm), M. Ličar (SI) 3.25, H. Tóth (HU) 2, A. Trojakova (CZ) 0.75, J. Sevcik (CZ) 2.75, , F. Meier (AT) 0.25, A. Bučánek (CZ) 3.25, R. Brožková (CZ) 0.75

Documentation: /

Status: ONGOING

Documents and publications

Publications:

Stay reports:

- A. Bučánek, 2026/03: ALARO + SURFEX surface DA workflow design (Should be published in ACCORD Newsletter)

DA contribution of RC LACE to the All Staff Workshop

6th All Staff Workshop, 13–17 April 2026, Marrakech

List of presentations:

- BUČÁNEK Antonín: Overview of LACE DA activities

National posters: Austria, Croatia, Czech Republic, Hungary, Slovakia, Romania, Slovenia

https://drive.google.com/drive/folders/10KvCsZq6alXWmhatMTzPtizqU8vlLD1j

Activities of management, coordination and communication

1) Attendance to 6th All Staff Workshop, 13.–17. April 2026, Marrakech
2) Attendance to EUMETSAT Core NWP meeting, online.
3) Attendance to OPERA Workshop, online. 30.1.2026
4) Attendance to Tactus WW, Brussels, 26.–29. May 2026
5) Attendance to ACCORD Surface WW at Prague, 18.–22. May 2026
6) Attendance to Accord DAWW preparation meetings, online.
7) Organization of informal LACE DA meetings (2nd Wednesday every two months), online.
8) ACCORD DA RD topical meetings, online.
9) LSC meetings.

Summary of resources

Action (PM)	Resource		LACE stays (months)	
	Planned	Realized	Planned	Realized
Operational implementation of DA suites [COM3]	8.0	4.00		
In-situ observations [DA1]	6.5	10.50	0.50	0.50
Use of ground-based remote sensing [DA2]	14.5	9.25	2.25	1.75
Satellite-based remote sensing observations [DA3]	19.0	10.00	1.75	0.00
Observation pre-processing, quality control, bias correction and representation error [DA4]	0.0	0.0		
Variational assimilation systems [DA5]	12.0	5.50		
EnVar, EDA and variants [DA6]	11.0	6.50		
Initialization methods and nowcasting [DA7]	0.0	0.00		
Diagnostic methods, optimization of assimilation cycling [DA8]	1.5	0.00		
AI/ML methods for data assimilation [DA9]	0.0	0.00		
Surface assimilation [SU1]	19.0	13.00	2.00	1.00
Total	**91.5**	**58.75**	6.50	3.25